

Water restrictions under climate change: a Rhone-Mediterranean perspective combining ‘bottom up’ and ‘top-down’ approaches”

Sauquet et al.

Anonymous Referee #2

The second version of the manuscript HESS-2018-456 has been significantly improved with respect to several technical issues related to the methodology.

However, I have still some doubts on the WRL modeling results, showing a higher consistency of the hydrological monitoring indicators with the adopted legally-binding water restrictions (WR) when modelled discharges (GR6J) are used as input, rather than when observed discharges (HYDRO) are considered (lines 364-371). Maybe, the calculation of WRLs as the median of the water restriction levels $wrl(d)$ for each 10-day period is not a good choice. Have you tried with different statistics, such as the mode? Otherwise, looking at Figure 6, one might think that the hydrological monitoring indicators alone are not enough to explain the reason for the implementation or non-implementation of WRs in some of the investigated catchments in the past years. For instance, negative deviations can derive from an increase in water demands (following section 4.5 changes in water demand are disregarded in this study), whereas positive deviations can be due to the availability of other water sources, such as groundwater or water storage in reservoirs.

➔ A discussion was introduced specifically on this aspect in Section 4.3. *“Heterogeneity in basin characteristics and rules imposed by the DMPs should not result in a systematic difference in Sensitivity and Specificity score between GR6J and HYDRO identified for most of the 15 evaluation catchments. Simulations were made on near pristine catchments and thus water uses are unlikely to be the main reason. Other causes of higher Sensitivity scores obtained when simulated discharges are used as input have been investigated in the WRL modeling framework. However, results of this analysis have not been conclusive. The aforementioned tests with the four prevalent modalities have all led to higher Sensitivity score using GR6J and higher Specificity score using HYDRO, demonstrating that the choice of the monitoring indicator and regulatory thresholds is probably not involved. A “smoothing” introduced by the hydrological modelling was also suspected but autocorrelation in observed and GR6J simulated VC3 time series was found very similar. Future works may re-investigate these aspects. They will need to explore new ones (e.g., the way WRL is derived from the daily values wrl for each 10-day period) using a longer verification period with not necessary uniform but fixed regulatory framework. Indeed some catchments have experienced only three years with legally-binding water restrictions and DMP have been frequently during the 2005-2013 period (see the black vertical segments in Fig. 6).”*

A new comment was added on the comparison between results obtained by HYDRO and GR6J. *“Using GR6J is more effective for detecting legally-binding restriction than using observed discharges while it is less efficient for predicting periods without restriction for most of the catchments. There is a compensatory effect, which is not easy to detect graphically since Sensitivity scores are more sensitive than Specificity scores due to the reduced number of observed days with adopted restrictions.”*

Technical revisions

Lines 68-69: “... in terms of vulnerability to climate change in terms of access to water for agricultural uses.” Please rephrase.

➔ The sentence has been modified: *“aims to establish a ranking of areas vulnerable to climate change in terms of water access for agricultural uses.”*

42 Line 173: Vcd is defined as a mean discharge, however I think it should be divided by the duration d , otherwise it
43 is a flow volume. → The definition of the mean discharge Vcd has been modified: $Vcd(t) = \frac{1}{d} \int_{t-d+1}^t Q_{daily}(t') dt'$

44 Line 193-195: “Where appropriate, other supporting local observations such as groundwater levels, reservoir water
45 levels, field surveys provided by the ONDE network (Beaufort et al., 2018) or feedbacks from stakeholders can be
46 used to inform final decisions.” → The sentence has been modified.

47 Line 231: “In the case of our study, this would be acceptable or not water restrictions for users,”. Something is
48 missing in this sentence. → The sentence has been clarified: “*In the case of our study, these thresholds will make*
49 *it possible to distinguish duration of water restrictions, which are unacceptable for users.*”

50 Line 295: what do you mean with “naturalized discharges”? → “*No routine to simulate water management (e.g.,*
51 *reservoir) was considered here since discharges of the 106 gauging stations are weakly altered by human actions*
52 *or naturalized discharges (i.e. flows corrected from the effects of water use).*”

53

54 **Water restrictions under climate change: a Rhone-**
55 **Mediterranean perspective combining ‘bottom up’ and ‘top-**
56 **down’ approaches**

57 Eric SAUQUET¹, Bastien RICHARD^{1,2}, Alexandre DEVERS¹, Christel PRUDHOMME^{3,4,5}

58

Correspondance to: E. Sauquet (eric.sauquet@irstea.fr)

59 ¹ Irstea, UR Riverly, 5 rue de la Doua CS20244, 69625 Villeurbanne cedex, France

60 ² Irstea, UMR G-EAU, Water resource management, Actors and Uses Joint Research Unit, Campus Agropolis -
61 361 rue Jean-François Breton – BP 5095, 34196 Montpellier Cedex 5, France

62 ³ European Centre for Medium-Range Weather Forecasts, Reading, UK

63 ⁴ Department of Geography, Loughborough University, Loughborough, LE11 3TU, UK

64 ⁵ NERC Centre for Ecology & Hydrology, Maclean Building, Benson Lane, Crowmarsh Gifford, Wallingford,
65 Oxon, OX10 8BB, UK

66 **Abstract** Drought management plans (DMPs) require an overview of future climate conditions for ensuring long-
67 term relevance of existing decision-making processes. To that end, impact studies are expected to best reproduce
68 decision-making needs linked with catchment intrinsic sensitivity to climate change. The objective of this study is
69 to apply a risk-based approach through sensitivity, exposure and performance assessments to identify where and
70 when, due to climate change, access to surface water constrained by legally-binding water restrictions may
71 question agricultural activities. After inspection of legally-binding water restrictions (WR) from the DMPs in the
72 Rhône-Méditerranée (RM) district, a framework to derive WR durations was developed based on harmonized low-
73 flow indicators. Whilst the framework could not perfectly reproduce all WR ordered by state services, as deviations
74 from socio-political factors could not be included, it enabled to identify most WRs under current baseline, and to
75 quantify the sensitivity of WR duration to a wide range of perturbed climates for 106 catchments. Four classes of
76 responses were found across the RM district. The information provided by the national system of compensation to
77 farmers during the 2011 drought was used to define a critical threshold of acceptable WR, related to the current
78 activities over the RM district. The study finally concluded that catchments in mountainous areas, highly sensitive
79 to temperature changes, are also the most predisposed to future restrictions under projected climate changes
80 considering current DMPs, whilst catchments around the Mediterranean Sea were found mainly sensitive to
81 precipitation changes and irrigation use was less vulnerable to projected climatic changes. The tools developed

82 enable a rapid assessment of the effectiveness of current DMPs under climate change, and can be used to prioritize
83 review of the plans for those most vulnerable basins.

84 **Keywords** Climate change; drought management plan; low-flow; France; scenario-neutral approach; response
85 surface; vulnerability; water restriction.

86 **1 Introduction**

87 The Mediterranean region is known as one of the “hot spots” of global change (Giorgi 2006; Paeth *et al.* 2017)
88 where environmental and socio-economic impacts of climate change and human activities are likely to be very
89 pronounced. The intensity of the changes is still uncertain, however, climate models agree on significant future
90 increase in frequency and intensity of meteorological, agricultural and hydrological droughts in Southern Europe
91 (Jiménez Cisneros *et al.* 2014; Touma *et al.* 2015), with climate change likely to exacerbate the variability of
92 climate with regional feedbacks affecting Mediterranean-climate catchments (Kondolf *et al.* 2013). Facing more
93 severe low-flows and significant losses of snowpack, southeastern France will be subject to substantial alterations
94 of water availability: Chauveau *et al.* (2013) have shown a potential increase in low-flow severity by the 2050’s
95 with a decrease in low-flow statistics to 50% for the Rhône River near its outlet. Andrew and Sauquet (2017) have
96 reported that global change will most likely result in a decrease in water resources and an increase both in pressure
97 on water resources and in occurrence of periods of water limitation within the Durance River basin, one of the
98 major water tower of southeastern France. In addition, Sauquet *et al.* (2016) have suggested the need to open the
99 debate on a new future balance between the competing water uses. More recently, based on climate projections
100 obtained from Coupled Model Intercomparison Project Phase 5 (Taylor *et al.* 2012), Dayon *et al.* (2018) have
101 shown a significant increase in hydrological drought severity with a meridional gradient (up to -55% in southern
102 France for both the annual minimum monthly flow with a return period of 5 years and the mean summer river
103 flow) while a more uniform increase in agricultural drought severity is projected over France for the end of the
104 21st century.

105 The challenges associated with possible impact of climate change on droughts have received increasing attention
106 by researchers, stakeholders and policy makers in the last decades. To date climate change impact studies are
107 usually dedicated to water resources (e.g., Vidal *et al.* 2016, Collet *et al.* 2018, Hellwig and Stahl 2018, Samaniego
108 *et al.* 2018) or water needs for the competing users (e.g., Bisselink *et al.*, 2018). However, examining the suitability
109 of regulatory instruments, such as Drought Management Plans, is also essential to establish successful adaptation

110 strategies. These plans state which type of water restrictions should be imposed to non-priority uses during severe
111 low-flow events; under climate change, those water restrictions and stakeholders' access to water resources might
112 need to be revised as drought patterns and severity might change. In most climate change impact studies, analyses
113 on the regulatory measures are often limited to maintaining environmental flows – especially when assessing future
114 hydropower potential. To date, no climate change impact on water regulatory measures have yet been assessed at
115 the regional scale, highlighting a gap in developing robust adaptation plans. This study aims to address this gap by
116 suggesting a framework, applying it to southeastern France and publishing the associated results.

117 The paper develops a framework to simulate legally-binding water restrictions (WR) under climate change in
118 the Rhone-Méditerranée district (southeastern France) and to assess the likelihood of future restrictions depending
119 on their sensitivity, performance and exposure to climate deviations. The approach is adapted from the risk-based
120 approaches such as developed in parallel by Brown *et al.* (2011) –named “Decision Tree Framework” –and
121 Prudhomme *et al.* (2010) –named “Scenario neutral approach”–and aims to establish a ranking of areas vulnerable
122 to climate change in terms of water access for agricultural uses in terms of vulnerability to climate change in terms
123 of access to water for agricultural uses. This research is a scientific contribution to the ongoing decade 2013–2022
124 entitled “Panta Rhei – Everything Flows” initiated by the International Association of Hydrological Sciences and
125 more specifically to the “Drought in the Anthropocene” working group ([https://iahs.info/Commissions--W-](https://iahs.info/Commissions--W-Groups/Working-Groups/Panta-Rhei/Working-Groups/Drought-in-the-Anthropocene.do)
126 [Groups/Working-Groups/Panta-Rhei/Working-Groups/Drought-in-the-Anthropocene.do](https://iahs.info/Commissions--W-Groups/Working-Groups/Panta-Rhei/Working-Groups/Drought-in-the-Anthropocene.do), Van Loon *et al.* 2016).
127 Legally-binding water restrictions and their associated decision-making processes are important for the blue water
128 footprint assessment at the catchment scale.

129 The paper is organized in four parts. Sect. 2 introduces the area of interest and the source of data. Sect. 3 is a
130 synthesis of the mandatory processes for managing drought condition implemented within the Rhône-Méditerranée
131 district and the related water restriction orders adopted over the period 2005-2016. Sect. 4 describes the general
132 modelling framework developed to simulate WR decisions. The approach is implemented at both local and
133 regional scales and results discussed in Sect. 5 before drawing general conclusions in Sect. 6.

134 **2 Study area and materials**

135 **2.1 Study area**

136 The Rhone-Méditerranée district covers all the Mediterranean coastal rivers and the French part of the Rhône
137 River basin, from the outlet of Lake Geneva to its mouth (Fig. 1). Climate is rather varied with a temperate

138 influence in the north, a continental influence in the mountainous areas and a Mediterranean climate with dry and
139 hot summers dominating in the south and along the coast. In the mountainous part (in both the Alps and the
140 Pyrenees) the snowmelt-fed regimes are observed in contrast to the northern part under oceanic climate influences,
141 where seasonal variations of evaporation and precipitation drive the monthly runoff pattern (Sauquet *et al.* 2008).

142 Water is globally abundant but unevenly between the mountainous areas, the northern and southern parts of the
143 Rhône-Méditerranée (RM) district and water resources are under high pressure due to water abstractions. For the
144 period 2008-2013, annual total water withdrawal was around 6 billion of m³ in the (excluding any water abstraction
145 for energy such as cooling nuclear plants and hydropower) with a more than used for irrigation (3.4 billion of m³,
146 including 2 billion of m³ for channel conveyance). Use for public and industrial supply is of 1.6 and 1 billion of
147 m³, respectively. Because of an intense competition for water between different users — agricultural, municipal,
148 and industrial — and the environment, some areas within the RM district can be vulnerable during low-flow
149 periods. Around 40% of the RM district suffers from water stress and scarcity ([http://www.rhone-](http://www.rhone-mediterranee.eaufrance.fr/gestion/gestion-quantite-problematique.php)
150 [mediterranee.eaufrance.fr/gestion/gestion-quantite-problematique.php](http://www.rhone-mediterranee.eaufrance.fr/gestion/gestion-quantite-problematique.php)) and has been identified by the French RM
151 Water Agency as areas with persistent imbalance between water supply and water demand.

152 **2.2 Drought management plan**

153 Drought management plans (DMPs) define specific actions to be undertaken to enhance preparedness and
154 increase resilience to drought. In France DMPs include regulatory frameworks to be applied in case of drought,
155 named “arrêtés cadres sécheresse”. The past and operating DMPs and the water restriction orders were inspected
156 in the 28 departments of the RM district. They were obtained from:

- 157 - The database of the DREAL Auvergne-Rhône-Alpes (“Direction Régionale de l’Eau, de l’Alimentation et du
158 Logement” in French) including WR levels and duration at the catchment scale available over the period 2005-
159 2016 within the RM district;
- 160 - The online national database PROPLUVIA (<http://propluvia.developpement-durable.gouv.fr>) with WR levels
161 and dates of adoption at the catchment scale for the whole France available from 2012.

162 The most recent consulted documents date from January 2017.

163 **2.3 Hydrological data**

164 The hydrological observation dataset is a subset of the 632 French near-natural catchments identified by
165 Caillouet *et al.* (2017). Daily flow data from 1958 to 2013 were extracted from the French HYDRO database

166 (<http://hydro.eaufrance.fr/>). Time series with more than 30% of missing values or more than 30% of null values
167 were disregarded. Finally, the total dataset consist of 106 gauged catchments located in the RM district with minor
168 human influence and with high quality data. The selected catchments are benchmark catchments where near natural
169 drought events are observed and current water availability is monitored. Water can be abstracted from other nearby
170 streams.

171 A selection of 15 evaluation catchments (Table 1) were used to calibrate and to evaluate the Water Restriction
172 Level modelling framework (Sect. 4), selected because (i) they have complete records of stated water restriction,
173 including dates and levels of restrictions - which was not the case of other catchments, and (ii) they are located in
174 areas where water restriction decisions are frequent. To facilitate interpretation, the 15 catchments have been
175 ordered along the north-south gradient. The Ouche and Argens River basins (n°1 and 15 in Table 1) are the
176 northernmost and the southernmost gauged basins, respectively. The 15 catchments encompass a large variety of
177 river flow regimes according to the classification suggested by Sauquet *et al.* (2008) (see Appendix A) that can be
178 observed in the RM district (e.g., the Ouche (1 in Table 1, pluvial regime), Roizonne (3, transition regime) and
179 Argens (15, snowmelt-fed regime) River basins).

180 **2.4 Climate data**

181 Baseline climate data were obtained from the French near-surface Safran meteorological reanalysis (Quintana-
182 Seguí *et al.*, 2008; Vidal *et al.* 2010) onto an 8-km resolution grid from 1 August 1958 to 2013. Exposure data was
183 based on the regional projections for France (Table 2) available from the DRIAS French portal ([www.drias-](http://www.drias-climat.fr)
184 [climat.fr](http://www.drias-climat.fr), Lémond *et al.* 2011). Catchment-scale data were computed as weighted mean for temperature and sum
185 for precipitation based on the river network elaborated by Sauquet (2006).

186 **3 Operating Drought Management Plans in the Rhône-Méditerranée district**

187 The French Water Act amended on September 24, 1992 (decree n°92/1041) defines the operating procedures for
188 the implementation of drought management plan (DMP). Following the 2003 European heat wave, drought
189 management plans including water restrictions have been gradually implemented in France (MEDDE 2004). Water
190 restrictions fall within the responsibility of the prefecture (one per administrative unit or department), as mentioned
191 in article L211-3 II-1° of the French environmental code. Their role in drought management is to ensure that
192 regulatory approvals for water abstraction continuously meet the balance between water resource availability and
193 water uses including needs for aquatic ecosystems. *De facto*, legally-binding water restrictions have to fulfill three

194 principles: (i) being gradually implemented at the catchment scale in regard with low-flow severity observed at
195 various reference locations, (ii) ensuring users equity and upstream-downstream solidarity and (iii) being time-
196 limited to fix cyclical deficits rather than structural deficits. The prefecture is in charge of establishing and
197 monitoring the DMP operating in the related department.

198 Past and current drought management plans were analyzed to identify the past and current modalities of
199 application, the frequency of water restriction orders and the areas affected by water restrictions. Gathering and
200 studying the regulatory documents was a tedious in particular because of their lack of clear definition of the
201 hydrological variables used in the decision-making process.

202 This analysis shows that the implementation of the DMPs has evolved for many departments since 2003, e.g.,
203 with changes in the terminology and a national scale effort to standardize WR levels. Now severity in low-flows
204 is classified into four levels, which are related to incentive or legally-binding water restrictions. These measures
205 affect recreational uses, vehicle washing, lawn watering and domestic, irrigation and industrial uses (Table 3).
206 Level 0 (named “vigilance”) refers to incentive measures, such as awareness campaign to promote low water
207 consumption from public bodies and general public. Levels 1 to 3 are incrementally legally-binding restriction
208 levels; level 1 (named “alert”) and 2 (named “reinforced alert”) enforcing reductions in water abstraction for
209 agriculture uses, or several days a week of suspension; level 3 (named “crisis”) involves a total suspension of water
210 abstraction for non-priority uses, including abstraction for agricultural uses and home gardening, and authorizes
211 only water abstraction for drinking water and sanitation services. Due to change in the naming of WR levels since
212 their creation one task was dedicated to restate the WR decisions (hereafter “OBS”) since 2005 with respect to the
213 current classification into four WR levels.

214 For all catchments, a WR decision chronology was derived, showing a large spatial variability in WR (Fig. 1) -
215 note that the 15 evaluation catchments (Table 1) are located in the most affected areas. Between 2005 and 2012,
216 WR decisions were mainly adopted between April and October (98% of the WR decisions, Fig. 2), with 62% in
217 July or August, peaking in July.

218 Decisions for adopting, revoking or upgrading a WR measure are taken after consultation of “drought
219 committees” bringing the main local stakeholders together, the meeting frequency of which is irregular and
220 depends on hydrological drought development. The adopted restriction level is mainly based on the existing
221 hydrological conditions at the time, *i.e.*, based on low-flow monitoring indicators measured at a set of reference

222 gauging stations and their departure from a set of regulatory thresholds. This varies greatly across the RM district
223 (Fig. 3). The low-flow monitoring indicators usually considered are:

- 224 - the daily discharge Q_{daily} ,
- 225 - the maximum discharge QCd , for a window with length d days, $QCd(t)=\max(Q_{daily}(t'),t'\in[t-d+1,t])$ and
- 226 - the mean discharge VCd , for a window with length d days, $VCd(t)=\frac{1}{d}\int_{t-d+1}^t Q_{daily}(t')dt'$.

227 Both QCd and VCd are computed over the whole discharge time series on moving time windows with duration
228 d associated with WR decision varying between 2 and 10 days depending on DMPs. $VC3$ (40% of DMPs) and
229 $QC7$ (17% of DMPs) are the most commonly used, but other single indicators include Q_{daily} (17%), $QC5$ (14%),
230 $QC10$ (8%), $QC2$ (3%), $VC10$ (3%), and with mixed indicators also used (e.g., 14% of $VC3$ and Q_{daily} together).

231 The threshold associated with WR also varies within the district, generally associated with statistics derived
232 from low-flow frequency analysis, but also fixed to locally-defined ecological requirements. In the context of
233 DMPs, series of minimum QCd or VCd are calculated by the block minima approach and thereafter fitted to a
234 statistical distribution. The block is not the year but the month or given by the division of the year into 37 10-
235 day time-window. The regulatory thresholds are given by quantiles with four different recurrence intervals
236 associated to the four restriction levels. Generally, return periods T of 2, 5, 10 and 20 years are associated with
237 the “vigilance”, “alert”, “reinforced alert” and “crisis” restriction levels, respectively. For example, let us
238 consider thresholds based on the annual monthly minima of $VCNd$. The block minima approach is carried out
239 on the N years of records for each month i , $i=1,\dots,12$ leading to twelve datasets $\{min\{VCNd(t), month(t)=i,$
240 $year(t)=j\}, j=1,\dots,N\}$. The twelve fitted distribution allows the calculation of 48 values of thresholds (=12
241 months \times 4 levels) with four T -year recurrence intervals.

242 The meteorological situation is also examined in terms of precipitation deficit and likelihood of significant
243 rainfall event considering available short to medium-range weather forecasts. There are heterogeneities in the
244 drought monitoring variables, the time period on which deficit is calculated and the permissible deviation from
245 long term average values.

246 Where appropriate, other supporting local observations such as groundwater levels, reservoir water levels,
247 field surveys provided by the ONDE network (Beaufort *et al.*, 2018) or feedbacks from stakeholders can be used
248 to inform final decisions.

249 Since their creation, DMPs have been frequently updated regarding the definition of the regulatory thresholds
250 and the monitoring variables, the water uses affected by legally-binding restrictions, the selection of the monitoring
251 sites, etc. It was especially done following the publication of the circular of the French ministry of Ecology in May
252 2011, and updates often occur after a year with a severe drought to include feedbacks and lessons for the future.
253 Decision-making processes is definitely heterogeneous in both time and space, which does not make the WR
254 modelling easy. In addition, official texts stating the DMPs were not all available for this study. Facing this
255 complexity, simplifying assumptions will be considered in the modelling framework presented in Section 4.3.4
256 Risk-based framework and the related tools.

257 **3 Risk-based framework and the related tools**

258 **4.1 The scenario neutral concept**

259 Traditionally, hydrological impact studies are often based on “top down” (scenario-driven) approaches, easy to
260 interpret, but with associated conclusions becoming outdated as new climate projections are produced. In addition
261 scenario-based studies may fail to match decision-making needs since the implication in terms of water
262 management is usually ignored (Mastrandrea *et al.* 2010). As a substitute to scenario-driven approach, the
263 scenario-neutral approach (Brekke *et al.* 2009, Prudhomme *et al.* 2010, 2013a, 2013b, 2015, Brown *et al.* 2012,
264 Brown and Wilby 2012, Culley *et al.* 2016, Danner *et al.* 2017) has been developed to better address risk-based
265 decision issues. The suggested framework shifts the focus on the current vulnerability of the system affected by
266 changes and on critical thresholds above which the system starts to fail to identify possible maladaptation strategies
267 (Broderick *et al.* 2019). Applied to water management issues, the scenario-neutral studies (e.g., Weiß 2011,
268 Wetterhall *et al.* 2011, Brown *et al.* 2011, Whateley *et al.* 2014) aim at improving the knowledge of the system’s
269 vulnerability to changes and at bridging the gap between scientists and stakeholders facing needs in relevant
270 adaptation strategy. Prudhomme *et al.* (2010) have suggested combining of the sensitivity framework with ‘top-
271 down’ projections through climate response surfaces. This approach has been applied to low-flows in the UK
272 (Prudhomme *et al.* 2015) and its interests have been discussed as a support tool for drought management decisions.

273 The risk-based framework adopted contains three independent components (Fig. 4):

- 274 (i) Sensitivity analysis (Fronzek *et al.*, 2010) based on simulations under a large spectrum of perturbed
275 climates to (a) quantify how policy-relevant variables respond to changes in different climate factors,
276 and (b) identify the climate factors to which the system is the most sensitive. Addressing (a) and (b)

277 may help modelers to check the relevance of their model (e.g., unexpected sensitivity to a climate factor
278 regarding the know processes influencing the rainfall-runoff transformation). From an operational
279 viewpoint, it may encourage stakeholders to monitor in priority the variables that affect the system of
280 interest (reinforcement of the observation network, literature monitoring, etc.),

281 (ii) Sustainability or performance assessment, aiming to identify under which climate (or other) conditions
282 (e.g., no rain period in spring, heat wave in summer, etc.) the system fails. A key-challenge in bottom-
283 up framework is to define performance metrics and associated critical thresholds relevant for the system
284 of interest. In the case of our study, these thresholds will make it possible to distinguish duration of
285 water restrictions, which are unacceptable for users.~~In the case of our study, this would be acceptable~~
286 ~~or not water restrictions for users,~~

287 (iii) Exposure, as defined by state-of-the-art regional climate trajectories superimposed to the climate
288 response surface. The exposure measures the probability of changes occurring for different lead times
289 based on available regional projections.

290 All the components of the framework together contribute to the vulnerability of the system (including its
291 management) to systematic climatic deviations.

292 The sensitivity analysis was conducted applying a water restriction modelling framework. Climate conditions
293 were generated applying incremental changes to historical data (precipitation and temperature) and introduced as
294 inputs in the developed models to derive occurrence and severity of water restriction under modified climates. The
295 tool chosen here to display the interactions between water restriction and the parameters that reflect the climate
296 changes is a two-dimensional response surface, with axes represented by the main climate drivers. This
297 representation is commonly used in scenario neutral approach. For example, in both Culley *et al.* (2016) and Brown
298 *et al.* (2012) the two axes were defined by the changes in annual precipitation and temperature. When changes
299 affect numerous attributes of the climate inputs, additional analyses (e.g., elasticity concept combined with
300 regression analysis (Prudhomme *et al.* 2015), Spearman rank correlation and Sobol' sensitivity analyses (Guo *et*
301 *al.* 2017)) may be required to point out the key variables with the largest influence on water restriction that form
302 thereafter the most appropriate axes for the response surfaces.

303 Performance assessment is a challenging task for hydrologists since it requires information on the impact of
304 extreme hydrometeorological past events on stakeholders' activities. Simonovic (2010) used observed past events
305 selected with local authorities on a case study in southwestern Ontario (Canada), chosen for their past impact

306 (flood peak associated with a top-up of the embankments of the main urban center; level II drought conditions of
307 the low water response plan). Schlef *et al.* (2018) set the threshold to the worst modelled event under current
308 conditions. Whateley *et al.* (2014) assessed the robustness of a water supply system and the threshold is fixed to
309 the cumulative cost penalties due to water shortage evaluated under the current conditions. Brown *et al.* (2012)
310 and Ghile *et al.* (2014) suggested selecting thresholds according to expert-judgment of unsatisfactory performance
311 of the system by stakeholders, whilst Ray and Brown (2015) use results from benefit-cost analyses. The spatial
312 coverage of a large area, such as the RM district, and the heterogeneity in water use (domestic needs, hydropower,
313 recreation, irrigation, etc.) makes it challenging for a systematic, consistent and comparable stakeholder
314 consultation to be conducted and for a relevant critical threshold T_c to be fixed for all the users. Facing this
315 complexity, only the irrigation water use will be examined here, since it is the sector which consumes most
316 water at the regional scale, with a critical threshold defined for this single water use.

317 Exposure to changes here is measured using regional projections, visualized graphically by positioning the
318 regional projections in the coordinate system of the climate response surfaces and identifying the associated
319 likelihood of failure relative to T_c . Note that, to update the risk assessment, only the exposure component has to
320 be examined (including the latest climate projections available onto the response surfaces).

321 **4.2 The rainfall-runoff modelling**

322 The conceptual lumped rainfall-runoff model GR6J was adopted for simulating daily discharge at 106 selected
323 catchments of the RM district. The GR6J model is a modified version of GR4J originally developed by Perrin *et*
324 *al.* (2003), well suited to simulate low-flow conditions (Pushpalatha *et al.* 2011). The 4-parameter version of the
325 model GR4J has been progressively modified. Lemoine (2008) has suggested a new groundwater exchange
326 function and a new routing store representing long-term memory in the GR5J model. Pushpalatha *et al.* (2011)
327 finally introduced in the GR6J model an exponential store in parallel to the existing store of the GR5J model.
328 Considering additional routing stores is consistent regarding the natural complexity of hydrological processes, and
329 in particular, the dynamics of flow components in low flows (Jakeman *et al.*, 1990).

330 The GR6J model has six parameters to be fitted (Fig. 5): the capacity of soil moisture reservoir (X1) and of the
331 routing reservoir (X3), the time base of a unit hydrograph (X4), two parameters of the groundwater exchange
332 function F (X2 and X5) and a coefficient for emptying exponential store (X6). The GR6J model is combined here
333 with the CemaNeige semi-distributed snowmelt runoff component (Valéry *et al.* 2014). The catchment is divided

334 into five altitudinal bands of equal area on which snowmelt and snow accumulation processes are represented. For
335 each band, daily meteorological inputs – including solid fractions of precipitation - are extrapolated using elevation
336 as covariate and the snow routine is calculated separately. Finally, its outputs are then aggregated at the catchment
337 scale to feed GR6J. The two parameters of ~~CemaNeige~~ CemaNeige S1 and S2 control the snowpack inertia and the
338 snowmelt, respectively. S1 is used to compute the thermal state of the snow pack eTG , which is an equivalent to
339 the internal snowpack temperature ($^{\circ}\text{C}$). $eTG(t)$ at day t is a weighted linear combination of the value of $eTG(t-1)$
340 ($\times S1$) and the air temperature at the day t ($\times(1-S1)$). S2 is the snowmelt degree-day factor used to calculate the
341 daily snowmelt depth by multiplying the air temperature when it exceeds 0°C , with S2. The splitting coefficient
342 of effective rainfall between the two stores (SC, in Fig. 5) has been fixed to 0.4 by Pushpalatha *et al.* (2011) since
343 calibrating SC lead to only slight better performance. The allocation of the outflow from the soil moisture reservoir
344 in 90% as percolation and 10% as surface and sub-surface runoff in the GR6J model is the results of previous
345 studies. The GR6J model was selected for its good performance across a large spectrum of river flow regimes
346 (e.g., Hublart *et al.* 2016, Poncelet *et al.* 2017).

347 No routine to simulate water management (e.g., reservoir) was considered here since discharges of the 106
348 gauging stations are weakly altered by human actions or naturalized discharges (*i.e.* flows corrected from the
349 *effects of water use*). The eight parameters (six from the GR6J model and two from the CemaNeige module) were
350 calibrated against the observed discharges using the baseline Safran reanalysis as input data and the Kling–Gupta
351 efficiency criterion (Gupta *et al.* 2009) KGE_{SQRT} calculated on the square root of the daily discharges as objective
352 function. The KGE_{SQRT} criterion was used to give less emphasis of extreme flows (both low and high flows). As
353 the climate sensitivity space includes unprecedented climate conditions (including colder climate conditions
354 around the current-day condition), the CemaNeige module was run for all the 106 catchments even for those not
355 currently influenced by snow.

356 The two step procedure suggested by Caillouet *et al.* (2017) was adopted for the calibration: first the eight free
357 parameters were fitted only for the catchments significantly influenced by snowmelt processes – *i.e.*, when the
358 proportion of snowfall to total precipitation $> 10\%$ - and second, for the other catchments, the medians of the
359 CemaNeige parameters were fixed and the six remaining parameters are then calibrated. Calibration is carried out
360 over the period 1 January 1973 to 30 September 2006 with a 3-year spin-up period to limit the influence of reservoir
361 initialization on the calibration results. The criterion KGE_{SQRT} and the Nash-Sutcliffe efficiency criterion on the
362 log transformed discharge NSE_{LOG} (Nash and Sutcliffe 1970) were calculated over the whole period 1958-2013

363 for the subset of 15 evaluation catchments (Table 1), showing KGE_{SQRT} and NSE_{LOG} values are above 0.80 and
364 0.70 respectively. These two goodness-of-fit statistics indicate that GR6J adequately reproduces observed river
365 flow regime, from low to high flow conditions. The less satisfactory performances of GR6J are observed for the
366 Tarn and Roizonne River basins, both characterized by smallest drainage areas and highest elevations of the
367 dataset. These lowest performances are likely to be linked to their location in mountainous areas (snowmelt
368 processes are difficult to reproduce) and to their size (the grid resolution of the baseline climatology fails to capture
369 the climate variability in the headwaters).

370 4.3 The water restriction level modelling framework

371 The Water Restriction Level (WRL) modelling framework developed aims to identify periods when the
372 hydrological monitoring indicator is consistent with legally-binding water restrictions. Only physical components
373 (mainly hydrological drought severity) leading to WR decisions are considered, with no socio-political factor
374 accounted for to model water restrictions.

375 To enable comparison of results across all catchments – in particular to combine response surfaces obtained
376 from different catchments (see Section 5.1) - the same drought monitoring indicators and regulatory thresholds
377 were adopted in all the catchments (see Section 3 for details), selected as most commonly used in the 28 DMPs
378 across the RM district, specifically $VC3$ as monitoring indicator and $10d-VCN3$ with return periods T of 2, 5, 10
379 and 20 years as regulatory thresholds. Each regulatory threshold is defined for a 10-day calendar period between
380 1st April and 31st October, resulting in 21 sets of four thresholds. Water restrictions are decided after consulting
381 drought committees that convene irregularly depending on hydrological conditions over a time window, *i.e.* the
382 last N days. Here a time window for analysis of $N= 10$ days was decided, which is consistent with the prefectural
383 decision-making time frame (frequency of updates in water restriction statements). The WRL modelling time-step
384 is finally fixed to 10 days and a representative value of WRL is given to the 21 10-day calendar periods from April
385 to October. Thus WRL is thus computed as follows:

- 386 - $VC3(t)$ is computed from daily discharge $Q_{daily}(t)$ every day t ;
- 387 - $VC3(t)$ is compared to the corresponding regulatory thresholds to create time series of daily water
388 restriction level wrl , with $wrl(t)$ ranging from 0 ('no alert') to 3 ('crisis'):
 - 389 ○ if $10d-VCN3(2) \geq VC3(t) > 10d-VCN3(5)$, $wrl(t)=0$
 - 390 ○ if $10d-VCN3(5) \geq VC3(t) > 10d-VCN3(10)$, $wrl(t)=1$

- 391 ○ if $10d\text{-VCN3}(10) \geq VC3(t) > 10d\text{-VCN3}(20)$, $wrl(t)=2$
- 392 ○ if $10d\text{-VCN3}(20) \geq VC3(t)$, $wrl(t)=3$
- 393 - A $WRL(d)$ time series is created as the median of $wrl(t)$ for each 10-day period;
- 394 - The $WRL(d)$ value is set to zero if preceding 10-day precipitation total exceeds 70% of inter-annual
- 395 precipitation average(precipitation correction).

396 Inputs of the WRL model are daily discharges and precipitation. Outputs are WRL time series with values for each
 397 21 10-day calendar period from April to October. Modelling is only applied to the period April-to-October, the
 398 irrigation period and when most water restrictions are put in place. The low-flow monitoring indicator $VC3$ and
 399 the regulatory thresholds $10d\text{-VCN3}(T)$ are computed from daily discharge time series Q_{daily} based on full period
 400 of records prior to 31st December 2013. The log-normal distribution is used to assess the return periods.

401 The WRL modelling framework can be applied to both observed and simulated time series. For the later, outputs
 402 from GR6J are used for simulations under current and modified climate conditions. Regulatory thresholds are
 403 derived from simulated discharge using the Safran baseline meteorological reanalysis as input, to moderate the
 404 possible effect of bias in rainfall-runoff modelling.

405 The WRL modelling framework was verified in the 15 evaluation catchments (Table 1). WRL simulations based
 406 on modelled (hereafter “GR6J”) and observed (hereafter ‘HYDRO’) discharge were compared graphically to
 407 official WR measures (“OBS”). A further assessment was conducted using the *Sensitivity* and *Specificity* scores
 408 (Jolliffe and Stephenson, 2003) to examine how well the WRL modelling framework can discriminate WR severity
 409 levels (Table 4). The *Sensitivity* score assesses the probability of event detection; the *Specificity* score calculates
 410 the proportion of “No” events that are correctly identified. An event was defined as any legally-binding Water
 411 Restriction of at least level 1, and ‘non-event’ a period where WRL is 0 or without WR. Comparisons were made
 412 over the 2005-2013 period, corresponding to the common period of availability for OBS, HYDRO and GR6J.

413 Fig. 6 shows years with severe simulated WRLs (e.g., 2005 and 2011) and years with no or few simulated WRs
 414 (e.g., 2010 and 2013). Both GR6J and HYDRO simulations are generally consistent with OBS, even if misses are
 415 found (e.g., basins 9 to 11 during the year 2005). There is no systematic bias, with some overestimations (e.g.,
 416 2005 using GR6J in basins 1 and 15; 2007 using HYDRO in basin 15), underestimations (e.g., 2009 in basin 6, 7,
 417 and 8) and misses (e.g., 2005 using HYDRO in basin 1).

418 *Sensitivity* and *Specificity* scores computed with OBS considered as benchmark (Fig. 7) show a large variation
419 across the catchments, in particular for *Sensitivity*. *Specificity* scores are around 0.85 for both GR6J and HYDRO,
420 suggesting that more than 85% of the observed non-events were correctly simulated by the WRL modelling
421 framework. The median of WRL *Sensitivity* score with HYDRO is around 45%, indicating that for half the
422 catchments, less than 45% of observed events are detected based on HYDRO discharges, but this raises to 68% of
423 events detected when WRLs are simulated based on GR6J discharge. Using GR6J is more effective for detecting
424 legally-binding restriction than using observed discharges while it is less efficient for predicting periods without
425 restriction for most of the catchments. There is a compensatory effect, which is not easy to detect graphically since
426 *Sensitivity* scores are more sensitive than *Specificity* scores due to the reduced number of observed days with
427 adopted restrictions. No evidence of systematic bias associated with catchment location or river flow regime was
428 found: northern (blue) and southern (red) catchments are uniformly distributed in the *Sensitivity/Specificity* space.

429 *Sensitivity* and *Specificity* scores using HYDRO as benchmark in the contingency table were also used to
430 compare simulations from GR6J discharge with those obtained from HYDRO discharge. Median values reach
431 84% (*Sensitivity*) and 92% (*Specificity*), showing high consistency between HYDRO and GR6J. No statistical link
432 between hydrological model and WRL model performance was found, with R^2 between NSE_{LOG} and *Sensitivity*,
433 or NSE_{LOG} and *Specificity* lower than 7%. In addition, the similar skill scores of GR6J and HYDRO modelling
434 suggest that possible biases in rainfall-runoff modelling does not impact on the ability of the WRL modelling
435 framework to correctly simulate declared or not declared WRs. ~~No evidence was found that the slightly higher~~
436 ~~*Sensitivity* scores for GR6J was due to a "smoothing" introduced by the hydrological modelling (similar~~
437 ~~autocorrelation between observed and GR6J simulated VC3 time series VC3), but the relatively short verification~~
438 ~~period (only three years with legally binding water restrictions in some catchments) and the frequency of DMP~~
439 ~~updates (black vertical segments in Fig. 6) might result in not truly representative scores.~~

440 Choosing the same definitions for the monitoring indicator and regulatory thresholds is a simplifying assumption
441 and may partly explain the deviations between simulated (HYDRO or GR6J) and adopted (HYDRO) WR
442 measures~~HYDRO and OBS~~. Before stating for VC3 and 10d-VCN3 the four prevalent modalities found in the
443 current DMPs have been tested to reproduce observed WR and results has shown a weak sensitivity to the
444 hydrological variables considered in the WR modelling framework. The mains reasons are that all the indicators
445 and thresholds are derived from *Qdaily* time series, are highly correlated and thus share, above all, the same
446 information on the dynamics and on the severity of drought.

447 Heterogeneity in basin characteristics and rules imposed by the DMPs should not result in a systematic difference
448 in *Sensitivity* and *Specificity* score between GR6J and HYDRO identified for most of the 15 evaluation catchments.
449 Simulations were made on near pristine catchments and thus water uses are unlikely to be the main reason. Other
450 causes of higher *Sensitivity* scores obtained when simulated discharges are used as input have been investigated in
451 the WRL modeling framework. However, results of this analysis have not been conclusive. The aforementioned
452 tests with the four prevalent modalities have all led to higher *Sensitivity* score using GR6J and higher *Specificity*
453 score using HYDRO, demonstrating that the choice of the monitoring indicator and regulatory thresholds is
454 probably not involved. A “smoothing” introduced by the hydrological modelling was also suspected but
455 autocorrelation in observed and GR6J simulated VC3 time series was found very similar. Future works may re-
456 investigate these aspects. They will need to explore new ones (e.g., the way WRL is derived from the daily values
457 wrl for each 10-day period) using a longer verification period with not necessary uniform but fixed regulatory
458 framework. Indeed some catchments have experienced only three years with legally-binding water restrictions and
459 DMP have been frequently during the 2005-2013 period (see the black vertical segments in Fig. 6).

460 Discrepancy between simulated and adopted WR measures is most likely due to the other factors involved in the
461 making-decision process. When regulatory thresholds are crossed, restrictive measures should follow the DMPs.
462 In reality, the measures are not automatically imposed, but are the result of a negotiating process. This process
463 includes for example some expert-judgment factors such as (i) the evolution of low-flow monitoring indicators
464 and thresholds over the years (e.g., annual revision for the Ouche, and irregular revision for the Isère (38), Gard
465 (30), Alpes-de-Haute-Provence (04) and Lozère (48) departments (last one in 2012)); (ii) the role of drought
466 committees in negotiating a delay in WR level applications to limit economic damages or to harmonize responses
467 across different administrative sectors sharing the same water intake; (iii) the local expertise especially regarding
468 the uncertainty in flow measurements (Barbier *et al.* 2007) impacting on the low-flow monitoring indicators, e.g.,
469 Cote d’Or (21) and Lozère (48) in the northern and southwestern parts of the RM district, respectively. Note that
470 where WR decisions are not uniquely based on hydrological indicators but also involve a negotiation process, the
471 results of the WRL modelling framework should be interpreted as potential hydrological conditions for stating
472 water restrictions.

473 Results of our sample study on 15 evaluation catchments show deviations for most catchments, but links between
474 order restrictions and hydrological drought severity. These deviations may partly be attributed to the use of the
475 same monitoring indicator and regulatory thresholds across the catchments in the modelling (whilst it is not true

476 in reality), as a necessary assumption for a region scale analysis. Tests with *QC7* as low-flow monitoring variable
 477 combined with the two dominant modalities for the regulatory thresholds show a weak sensitivity of the WRL
 478 modelling skill to the choice of the indicators (with a slight increase in *Specificity* score (~ 90%) while *Sensitivity*
 479 score is reduced (< 50%) using GR6J). Whilst the developed WRL modelling framework does not account for
 480 expert-decision brought by drought committees - and hence is not designed to simulate the exact WR decisions -
 481 its ability to simulate 68% of the stated restrictions over the period 2005-2013 demonstrates its usefulness as a tool
 482 to objectively simulate the potential of drought restrictions based on hydrological drought physical processes. The
 483 methodology was applied to the 106 catchments of the RM district under climate perturbations to assess the
 484 potential impact of climate change on water restriction in the region. The resulting analysis focuses on water
 485 restriction level higher than 1, denoted thereafter WR*.

486 4.4 The generation of perturbed climate conditions

487 The generation of climate response surfaces relies on synthetic climate time series representative of each explore
 488 climate condition, and used as input to the impact modelling chain (here hydrological model and WRL modelling
 489 framework). Methods based on stochastic weather simulation have been used (e.g., Steinschneider and Brown
 490 2013, Cipriani *et al.* 2014, Guo *et al.* 2016, 2017), but they can be complex to apply in a region with such
 491 heterogeneous climate as the RM district. Alternatively, the simple “delta-change” method (Arnell 2003) has been
 492 commonly used to provide a set of perturbed climates in scenario-neutral approach (e.g., Paton *et al.* 2013, Singh
 493 *et al.* 2014), and was used here, similarly to (Prudhomme *et al.* 2010, 2013a, 2013b, 2015).

494 Following Prudhomme *et al.* (2015), monthly correction factors ΔP and ΔT are calculated using single-phase
 495 harmonic functions:

$$496 \Delta P(i) = P_0 + A_P \cdot \cos \left[(i - \varphi_P) \cdot \frac{\pi}{6} \right]. \quad (1)$$

$$497 \Delta T(i) = T_0 + A_T \cdot \cos \left[(i - \varphi_T) \cdot \frac{\pi}{6} \right]. \quad (2)$$

498 with P_0 and $T_0 + A_T$ mean annual changes in precipitation (1) and temperature (2), respectively; i indicator of the
 499 month (from 1 to 12); φ_P the phase parameter and A_P the semi-amplitude of change (e.g., half the difference
 500 between highest and lowest values). These corrections factors were applied to the baseline climate data sets to
 501 create perturbed daily forcings:

$$502 P^*(d) = P(d) \cdot [\overline{PM}(\text{month}(d)) + \Delta P(\text{month}(d))] / \overline{PM}(\text{month}(d)) \quad (3)$$

503
$$T^*(d) = T(d) + \Delta T(\text{month}(d)) \quad (4)$$

504 with $P(d)$ and $T(d)$ baseline precipitation and temperature values for day d ; $P^*(d)$ and $T^*(d)$ the corrected (or
 505 perturbed) values for day d ; $\overline{PM}(\text{month}(d))$ average monthly baseline precipitation for $\text{month}(d)$. Corrected
 506 potential evapotranspiration PET^* time series were derived from temperature values using the formula suggested
 507 by Oudin *et al* (2005):

508
$$PET^*(d) = \max \left[PET(d) + \frac{Ra}{28.5} \frac{\Delta T(\text{month}(d))}{100}; 0 \right] \quad (5)$$

509 with $PET(d)$ baseline potential evapotranspiration values for day d ; Ra extra-terrestrial global radiation for the
 510 catchment.

511 The baseline climate (precipitation and temperature) time series were extracted from the Safran reanalysis over
 512 the period 1958-2013 (56 years), and perturbed time series generated for the same length. The range of climate
 513 change factors to generate the perturbed series were chosen to encompass both the range and the seasonality of
 514 RCM-based changes on projections in France. A set of 45 precipitation and 30 temperature scenarios was created
 515 (Fig. 8), spanning the range of potential future climate suggested by Terray and Boé (2013) and combined
 516 independently, resulting in a total of 1350 precipitation and temperature perturbations pairs used to define the
 517 climate sensitivity space. In this application,

- 518 - P_0 (mm.an⁻¹) = $-20 + 20/3 \times (j-1)$, $j= 1, \dots, 9$,
- 519 - A_p (mm.season⁻¹) = $20/3 \times (j-1)$, $j= 1, \dots, 5$,
- 520 - T_0 (°C.an⁻¹) = $j-1$, $j= 1, \dots, 6$,
- 521 - A_T (°C.season⁻¹) = $-0.5 + 2 \times (j-1)$, $j= 1, \dots, 5$,
- 522 - φ_P parameter is fixed to 1 to consider minimum change in January and maximum change in July and
- 523 - φ_T is fixed to 2 to get maximum change in August.

524 **4.5 The assumptions on water uses**

525 Water uses and the feedbacks between use and available resources are not explicitly addressed in this application,
 526 either under current or future conditions. This should not be considered as a limitation for basins where
 527 hydrological modelling has been implemented. Indeed, the 106 basins under study have been carefully chosen
 528 since they are currently little or not influenced by human actions. These catchments are benchmark catchments
 529 where natural water availability is monitored for the statement of restriction orders. Water can be abstracted from

530 other neighboring rivers. Water needs will probably evolve in the next decades. Water requirement for irrigation
531 may increase in parallel to air temperature or may decrease due to adaptive actions (e.g. farmers may choose to
532 plant specific crops less sensitive to water shortages). Water needs and sensitivity to water restrictions depend on
533 socio-economic and institutional pathways. Forward-looking studies have been recently carried out with the
534 involvement of local experts but at the local scale (Grouillet *et al.*, (2015) for the Hérault River basin; Andrews
535 and Sauquet, (2016) for the Durance River basin). The distinct underlying assumptions make difficult to combine
536 and to extend the prospective scenarios over the RM district. Thus, the water restriction modelling framework
537 considers, in this application, the “Business-as-usual” scenario, which assumes that only minor change in water
538 demand behavior will occur. In particular, no major alteration of the river flow regime is projected for the 106
539 catchments. Despite unrealistic, maintaining the current conditions allows assessing the impact of climate change
540 regardless of any other human-induced changes. The advantage is that results are easier to understand and to
541 embrace by stakeholders than those obtained with complex multi-sectorial scenarios they may not identify with.

542 **5 Drought management plans under climate change and their impact on irrigation use**

543 **5.1 The Water Restriction response surfaces**

544 The 1350 sets of perturbed precipitation, temperature and PET time series were each fed into the WRL modelling
545 framework for each 106 catchments. Both VC3 (monitoring indicators) and 10d-VCN3(T) (regulatory thresholds)
546 were computed from GR6J 56 years discharge simulations. For each scenario, the number of 10-day periods under
547 Water Restriction of at least level 1 (WR*) were calculated, and expressed as deviation from the simulated baseline
548 value: ΔWR^* , hence removing the effect of any systematic bias from the WRL modelling framework. Results are
549 shown as WR response surfaces built with x - and y -axes representing key climate drivers. Because different climate
550 perturbation combinations share the same values of the key climate drivers, hence represented at the same location
551 of the response surface, the median ΔWR^* from all relevant combinations is displayed as color gradient, with the
552 standard deviation Sd of ΔWR^* showed as size of the symbol.

553 Response surfaces based on different climate variables for x (precipitation) and y (temperature) were generated
554 over full or part of the water restriction period (April to October “AMJJASO”, March to June “MAMJ”; and July
555 to October “JASO”, the latter coinciding with the highest temperatures) and visually inspected to identify the
556 greatest signal pattern, combined with the smallest dispersion around the surface response (*i.e.*, analysis of the
557 median and the maximum of Sd values over the grid cells).

- 558 The response surfaces are exemplified on three of the 15 evaluation catchments (Table 1, Fig. 9):
- 559 - The Argens River basin, along the Mediterranean coast, severe low-flows occur in summer and actual
 - 560 evapotranspiration is limited by water availability in the soil,
 - 561 - The Ouche River basin, in the northern part of the RM district, has a typical pluvial river flow regime under
 - 562 oceanic climate influences, where runoff generation is less bounded by evapotranspiration processes,
 - 563 - The Roizonne River basin, in the Alps, typical of summer flow regime controlled by snowmelt, with spring
 - 564 to summer climate conditions dominating changes in low-flows.
- 565 The visual inspection of response surfaces shows that:
- 566 - ΔWR^* are differently driven by the changes in precipitation ΔP and in temperature ΔT : ΔWR^* is very
 - 567 sensitive to ΔP in the Argens River basin (horizontal stratification in the response surface) and to ΔT in the
 - 568 Roizonne River basin (vertical stratification in the response surface) whilst being controlled by both drivers
 - 569 in the Ouche River basin;
 - 570 - There is a high likelihood of increase in the duration of water restriction in the Roizonne River basin, as
 - 571 showed a response surface dominated by positive ΔWR^* ;
 - 572 - Sd values may vary significantly from one graph to another (Table 5). For both the Argens and Roizonne
 - 573 River basins, largest Sd are found when the response surfaces are displayed with climate variables computed
 - 574 over the whole period April-to-October (AMJJASO) while smallest Sd are associated with ΔP and ΔT
 - 575 drivers from March to June. Changes in mean spring to early summer precipitation and temperature mainly
 - 576 govern changes in WR^* for these two basins. Conversely changes in precipitation ΔP and temperature ΔT
 - 577 over the full period April-to-October seem the dominant drivers of changes in WR^* for the Ouche River
 - 578 basin.

579 **5.2 Response surface analysis at the regional scale**

580 Following (Köplin *et al.* 2012, Prudhomme *et al.* 2013a), the 106 response surfaces were classified to define

581 typical response surfaces, designed as tools to help prioritizing actions for adapting water management rules to

582 future climate conditions in the RM district. Here a hierarchical clustering based on Ward's minimum variance

583 method and Euclidian distance as similarity criteria (Ward 1963) was applied and four classes were identified after

584 inspection of the agglomeration schedule and silhouette plots (Rousseeuw 1987). A manual reclassification was

585 conducted for the few catchments with negative individual silhouette coefficients to ensure higher intra-class
586 homogeneity. For each class, a mean response surface and associated Sd was computed, and main climate drivers
587 associated with WR changes identified (Table 5).

588 All suggest an increase in the occurrence of legally-binding water restrictions when precipitation decreases or
589 when temperature increases (Fig. 10). Additional temperature increase and its associated PET increase can
590 compensate for precipitation increase and lead to decrease in ΔWR^* with intra-class differences emerging in the
591 magnitude of changes. The identified four typical Water Restriction response surfaces show a weak regional
592 pattern and common features. Class 4 (including the Roizonne River basin) regroups snowmelt-fed river flow
593 regimes in the Alps, whilst basins of Class 1 are mainly Mediterranean river flow regimes. Class 2 (including the
594 Ouche River basin) and Class 3 catchments are partly influenced by both precipitation and temperature, with
595 ΔWR^* in Class 2 catchments less sensitive to climatic changes (flatter WR response surface) than catchments of
596 Class 3. Flow regime of Classes 2 to 3 ranges from rainfall-fed regimes with high flow in winter and low flow in
597 summer in the northern part of the RM district to regimes partly influenced by snowmelt with high-flows in spring
598 in the Alps and in the Cevennes.

599 To further the regional analysis and help sensitivity assessment at un-modelled catchments, basin descriptors
600 were investigated as possible discriminators of the four classes. A set of potential discriminators - which included
601 measures of the severity, frequency, duration, timing and rate of change in low-flow events (Table 6), the drainage
602 area and the median elevation for the catchment and one climate descriptor (mean annual precipitation and mean
603 annual potential evapotranspiration used to compute an aridity index) – were introduced in a CART model
604 (Classification And Regression Trees, Breiman *et al.*, 1984), aimed at performing successive binary splits of a
605 given data set according to decision variables. Through a set of “*if-then*” logical conditions the algorithm
606 automatically identifies the best possible predictors of group membership, starting from the most discriminating
607 decision variable to the less important factors. The optimal choices are fixed recursively by increasing the
608 homogeneity within the two resulting clusters. At each step one of the clusters (node) is divided into two non-
609 overlapping parts. Here, to free results from catchment size influence, descriptors related to severity were
610 expressed in mm/year, mm/month or mm/day.

611 Results show three top discriminators, the aridity index being the strongest:

612 - Aridity index AI given by the mean annual precipitation divided by the mean annual potential
613 evapotranspiration (UNEP, 1993),

614 - Baseflow index *BFI*, a measure of the proportion of the baseflow component to the total river flow, calculated
615 by the separation algorithm separation suggested by Lyne and Hollick (1979),
616 - Concavity Index *IC* (Sauquet and Catalogne 2011) to characterize the contrast between low-flow and high-
617 flow regimes derived from quantiles of the flow duration curve,
618 CART overall misclassification (18%) suggests a satisfactory performance in classification method,
619 characterized by a parsimonious algorithm (five nodes and three variables) with potential for a first guess
620 assessment of the WR response to disruptions and evaluation of the robustness of existing water restriction at the
621 department-level scale. For each class, Fig. 11 shows the empirical distribution of the three main discriminators,
622 the mean timing θ of daily discharge below Q_{95} and its dispersion r , based on circular statistics, where Q_{95} is the
623 95th quantile derived from the flow duration curve.

624 The classification discriminates catchments primarily on the seasonality of low-flow conditions and the aridity
625 index, with the extreme classes (1 and 4) being particularly well discriminated.

626 Geographically, Class 1 catchments are mainly located along the Mediterranean coast and include the Argens
627 River basin; ΔWR^* is mainly driven by changes in precipitation in spring and early summer. Class 1 gathers water-
628 limited basins with small values of *AI* and a weak sensitivity to climate change in summer. In these dry water-
629 limited basins, the mid-year period exhibits the minimal ratio P/PET and changes in summer precipitation has
630 hence only a moderate impact on low-flows; spring is the only season when *PET* changes are likely to result in
631 both actual evapotranspiration and discharge changes. WR levels are more likely controlled by antecedent soil
632 moisture conditions in spring and early summer. This behavior is typical of the basins under Mediterranean
633 conditions and was discussed in the context of a scenario-neutral study in Australia (Guo *et al.* 2016). For those
634 catchments, climate drivers computed in spring (over the period MAMJ) are used to describe the x- and y-axes of
635 the response surface, fully consistent with water-limited basin processes.

636 Catchments of both Class 2 and 3 have similar *IC*, hence suggesting that flow variability is not a proxy for low-
637 flow response to climatic deviation. However, *BFI* values for Class 3 are lower than for Class 2 while Class 3 is
638 characterized by high values for *AI*. Despite higher capability to sustain low-flows (see *BFI* values) the response
639 surface representative of Class 2 is more contrasted than that of Class 3; a possible reason could be drier conditions
640 under current conditions (the median of *AI* equals 2.5 for Class 3 against 1.6 for Class 2). The monthly perturbation
641 factors (see Sect. 5.1) are the same for all the classes but the changes in relative terms are less significant regarding

642 the current climate conditions for Class 3 than for Class 2, and may explain the limited changes in river flow
643 patterns.

644 Class 4 regroups catchments with low flows in winter and significant snow storage. The *BFI* values are high and
645 due to smooth flow duration curves, *IC* demonstrates also high values.

646 **5.3 Risk assessment at the basin scale**

647 The risk-based framework has been applied to the irrigation water use since annual net total water withdrawal
648 for agriculture purposes is ranked first at the regional scale. Note that in the Rhône-Méditerranée district around
649 90% and 10% of water used for irrigation originate from surface water and groundwater, respectively. To
650 complement water needs irrigators may also have access to small reservoirs (storage capacity usually less than 1
651 Mm³). Most of the reservoirs are filled by surface water in winter and release water later in the following summer.
652 Water restrictions are not imposed to these reservoirs but it is assumed here that during severe drought events the
653 majority of them are empty and thus the existence of potential sources auxiliary to surface water on the conclusions
654 has limited influence on the conclusions.

655 We assumed here that irrigated farming is globally under failure if the duration with limited or suspended
656 abstraction is above a critical threshold T_c that causes insufficient water for crops. The catchment or area i will be
657 considered more vulnerable than the catchment or area j if the likelihood of failure (*i.e.*, exceeding T_c) for
658 catchment or area i is more than the likelihood of failure for catchment or area j . The critical threshold T_c is a value
659 of total number of days with legally-binding water restrictions that needs to be fixed. To move closer to reality and
660 following Simonovic (2010), the value of T_c is based on the analysis of past events. A possible way to fix T_c is to
661 simulate historic drought events observed during the period 2005-2012 and the effects of water restrictions on crop
662 yield and quality and on economic losses. Computing water deficits was considered rather tricky at the farming
663 scale - partly due to the high heterogeneity in crop and soil types, watering systems, conveyance efficiencies, etc.
664 across the RM district - and we have investigated the use of 'agricultural disaster' notifications as proxies to
665 identify the damaging conditions instead.

666 Specifically the 'agricultural disaster' notifications are issued by the agriculture ministry following
667 recommendations from the Prefecture to each department affected by extreme hydro-meteorological events, and
668 applied uniformly over the RM district. Whilst 'agricultural disaster' status is a global index that may mask
669 heterogeneity in crop losses within each department, and that reflects losses related to both agricultural and

670 hydrological droughts, it has the advantage of being directly related to economic impact, and uniformly applied
671 across the RM district, hence suitable for a regional-scale analysis. The national system of compensation to farmers
672 is initiated for areas notified under ‘agricultural disaster’ status.

673 Over 2005-2012, only one agriculture disaster was declared, in 2011, and applied to 70 of the 95 departments in
674 continental France, and to 16 of the 28 departments fully or partly located in the RM district. Data are collected
675 by the French Ministry of Agriculture and Food and they are not publically available. The year 2011 was the only
676 year when the national system of compensation has been triggered between 1958 and 2013 and the analysis of
677 simulated water restrictions for this year fixed the value for T_c . The duration of water restrictions was calculated
678 individually for each catchment and converted into anomalies $\Delta WR^*(2011)$ with respect to the benchmark value
679 (mean over the period 1958-2013). For consistency with the indicators used in the response surfaces, this threshold
680 $\Delta WR^*(2011)$ is derived from GR6J outputs.

681 The RCM-based projections of all the catchments of the class for the three time slices 2021-2050, 2041-2070
682 and 2071-2100 were superimposed to the representative response surfaces to assess the risk of failure (Fig. 4).
683 Finally the vulnerability resulting from the combination of the three components sensitivity, performance and
684 exposure was measured by the proportion of RCM-based projections leading to critical situations-, similarly to
685 Prudhomme *et al.* (2015). Technically this Vulnerability Index (VI) calculated as the proportion of exposure
686 simulations that fail below the critical threshold T_c is the complement to the “climate-informed” robustness index
687 (CRI) (Whateley *et al.*, 2014). Given one specific climate projection, a catchment or a group of catchments could
688 be judged vulnerable if on average T_c is exceeded. VI is introduced here to account for the uncertainty in climate
689 projections in risk assessment. This index should be interpreted as conditional probability (risk) with respect to a
690 specified ensemble of future climates.

691 Fig. 12 shows an application to the Ouche River basin, North of the RM district (1, Fig. 1, Table 1) and declared
692 under agricultural disaster status in 2011. The black dotted line are isopleths connecting points of the response
693 surface with $\Delta WR^* = \Delta WR^*(2011) = T_c$ (= 7 10-day periods for this catchment), and delimits the climate space
694 leading to median climatic situations more severe than 2011 ($\Delta WR^* > \Delta WR^*(2011)$, above left) or less severe than
695 2011 ($\Delta WR^* < \Delta WR^*(2011)$, below right) $\Delta WR^*(2011)$. As reference, the black solid line ($\Delta WR^* = 0$) delimits
696 the climate space associated with more (above left) or less (bottom right) water restrictions compared with the
697 whole period average (1958-2013). Basin-scale exposure projections (Table 2) were plotted onto the WR response

698 surface for three time-slices 2021-2050, 2041-2070 and 2071-2100 (grey symbols), showing a warmer trend but
699 no total precipitation signal. Whilst by the end of the century, projections move towards the critical threshold
700 $\Delta WR^*(2011)$ climate space, pointing out a significant increase in more severe low-flows, there remain a large
701 spread in signal (dispersion of the grey symbols) and the vulnerability index equals zero for this catchment.

702 **5.4 A regional perspective for prioritizing adaptation strategies**

703 Following the methodology applied to the Ouche River basin, $\Delta WR^*(2011)$ were calculated for individual
704 catchments and averaged to produce a value of T_c relevant for each Class (Table 7). Class variation in $\Delta WR^*(2011)$
705 is large, with Class 2 and 3 showing thresholds of at least 7 10-day periods, whilst they are close to zero for Class
706 1 and Class 4. The scatter in the $\Delta WR^*(2011)$ values is certainly due to heterogeneity in crops, in irrigation
707 systems, in climate conditions, etc. at the regional scale leading to locally differentiated sensitivity to water
708 restrictions as well as to biases in WR modelling. Since only the year 2011 it is now difficult to conclude on the
709 origins of the dispersion (natural or non-natural). However the distribution and absolute values of the critical
710 thresholds reflect well the spatial pattern of WR enforced from May to September 2011, with Southern regions
711 and the French Alps moderately affected by lack of rainfall in spring compared to the Northern and Western
712 regions of the RM district (Fig. 13). Surprisingly negative values for $\Delta WR^*(2011)$ are found for some catchments
713 of Classes 1 and 4, providing no evidence to support their agricultural disaster status that year. At the RM scale,
714 average $\Delta WR^*(2011)$ equals 38 days when considering all catchments, and increases to 66 days when considering
715 only catchments under agricultural disaster status. Simplifying but realistic assumptions are imposed by the lack
716 of detail information; thus only one value was considered at the regional scale despite high dispersion in
717 $\Delta WR^*(2011)$ values (Table 7): the critical threshold T_c was set to the average of the $\Delta WR^*(2011)$ values computed
718 on all catchments in departments under agricultural disaster status in 2011 (6.6 10-day periods), and was used
719 thereafter for all classes. Note that this value of T_c seems realistic: it represents a significant period with restrictions
720 (66 days or 30% of the time between the 1st April and the 31st October).

721 Using the Class WR response surface as diagnostic tools, exposure information (grey symbols) and thresholds
722 ($\Delta WR^*=0$, solid, $\Delta WR^*(2011)$, dashed black lines) were displayed (Fig. 14), and VI calculated (Table 7). The
723 location of the two isopleths $\Delta WR^* = \Delta WR^*(2011)$ (black dotted line) and $\Delta WR^* = 0$ (black straight line) in the
724 WR response surface depends on the shape of the response surface and differ from one class to another. The portion
725 of the WR response surface associated with $\Delta WR^* < 0$ is gradually lower from Class 1 to Class 4 suggesting that

726 catchments of Class 4 are more subject to an increase in water restriction occurrence than catchments of the other
727 classes. Classes 1 and 4, the most extreme responses classes, contain fewer catchments, whilst Classes 2 and 3,
728 characterized by an intermediate response, have the most of the catchments. Because of the large geographical
729 spread of catchments of Class 2 and 3, an expert-based division was done to distinguish catchments with
730 continental (northern sectors) and Mediterranean (southern sectors) climate in terms of exposure. This is to better
731 capture the predominantly north–south gradient in future projections of both temperature and rainfall, as they
732 differing impact on the river flow regime (e.g., Boé *et al.* 2009; Chauveau *et al.* 2013; Dayon *et al.* 2018). For all
733 classes, vulnerability increases with lead time, with Class 4 showing the largest vulnerability and Class 1 being
734 the less vulnerable despite its location in the Mediterranean area. In the two classes 2 and 3, vulnerability increases
735 from North to South in the RM district (e.g., $VI = 13\%$ for Class 2-N against 32.9% for Class 2-S at the end of the
736 century). These contrasted results are mainly explained by the difference between exposure characterizations since
737 a common value of the threshold T_c was adopted.

738 **5.4 Water restriction policy implementation**

739 In 2011, France adopted a general framework for action—the French National Climate Change Impact
740 Adaptation Plan (“Plan National d’Adaptation au Changement Climatique (PNACC)” in French)—with numerous
741 recommendations related to research and observation. Five priorities of the first PNACC related to water resources
742 have been highlighted. The PNACC has been recently reviewed and the PNACC2 published in December 2018
743 confirms the place of DMPs as tools for monitoring water resources and water allocation, and for driving greater
744 public and stakeholder awareness (<https://www.ecologique-solidaire.gouv.fr/adaptation-france-au-changement-climatique>).
745

746 However and until now, impacts of future climate change is not account for in DMPs. The development of DMPs
747 have helped to ease past conflicts at the department scale. Water users are now facing more frequent water
748 restrictions (more than half France have departments experiencing $WR \geq 1$ between 2011 and 2018 (Fig. 15)) and
749 the timing and the level of the restrictions vary from one year to another: the highest number of French departments
750 with $WR \geq 1$ was observed in summer in both 2015 and 2017 while the year 2018 was characterized by late water
751 restrictions (mostly in autumn). Stakeholders are now questioning the DMP implementation, but only at the short
752 term – the impact of climate change is not yet a subject matter. One of their main concerns is the heterogeneity in
753 current restrictions levels and timing from one department to another or from the upstream to the downstream part
754 of the catchment. One of the option being considered to address this challenge in southeastern France is to

755 harmonise the definition of the regulatory thresholds, at the regional scale. Results obtained here show that the
756 standardisation will probably not fix the problem due to the balance between socio-political and hydrological
757 factors in the final WR statement.

758 The map displaying the class membership could be a convenient tool for local authorities to discuss the spatial
759 heterogeneity in terms of impact to drought on water restrictions under both current and future climate conditions.
760 Despite operating rules uniformly applied, there is a high variability in catchments responses within the department
761 (see the southernmost department in Fig. 10). Therefore, any investigation on DMPs at the department level
762 disregarding this heterogeneity will be biased. The sensitivity analysis provides information for local authorities
763 to better understand the differences in catchment responses to observed droughts in areas, which fall within their
764 responsibility. For instance, water management in basins of Class 4 could be more problematic during a year with
765 a severe heat wave while it could be more problematic for a year with a pronounced precipitation deficit for
766 catchments of Class 1. It is likely that the differences in the impact of droughts on WR will persist if stakeholders
767 do not question the assumption of a uniform definition for the hydrological indicators within the department.

768 DMPs have been recognized in the PNACC as relevant water management tools and our findings have also
769 implications for adaptation strategies. We have shown that the climate change effects could be felt more acutely
770 during the irrigation period by an increase in water restriction. Thus, relying on surface water to compensate
771 deficits is highly hazardous. Options under consideration are saving water, enhancing water storage by building
772 new small dams or securing water access by transferring water from the Rhone River (e.g., Ruf, 2012), which is
773 considered as an “overabundant” river within the RM district. Saving water is the solution favoured by the RM
774 Water Agency. Creating new storages is increasingly considered as potential solution to secure water for
775 agriculture since they are not subject to water restrictions. Authorising new water storages may also reduce the
776 sense of unfairness among users in areas with no secured access. Most of the small reservoirs are filled by surface
777 water in winter, release water later in summer for irrigation purposes and then limit the pressure on water resource
778 during crises. However, there is actually a wide discussion about these hydraulic structures in France since their
779 cumulative impacts on the ecosystem and their efficiency are not well known (Habets *et al.*, 2018). Building
780 adaptation strategies on additional water storage may lead to maladaptation since natural inflows will probably
781 decrease, and delay the mutation of agricultural practices and conservation measures. In addition, there is actually
782 no guarantee that these reservoirs will be filled and that their storage capacity will be enough to cope with severe
783 droughts.

784 The RM Water Agency has taken other the objectives of PNACC at the regional scale and has initiated an
785 unprecedented major initiative that provides guidance for the River Basin Management Plan (2016–2021). The
786 adaptation strategy partly relies on an analysis of the vulnerability in different water-related sectors (water
787 resources, soil-moisture, biodiversity, and water quality) within the RM district to climate change. The study
788 complements this former analysis by focusing here on agricultural uses and meets the requirements for
789 vulnerability assessment carried out by the RM Water Agency: it covers the same area and the methodology is
790 uniformly applied across the area of interest. It may help the RM Water Agency identifying when and where
791 actions and investments are the most needed to mitigate the effects of climate change (probably in catchments of
792 Class 4 from the short perspective, and later for the other areas).

793 **6 Conclusions**

794 This paper presents a first attempt to analyse and simulate water restrictions over a large area in France applying
795 an alternative approach to the classical “top-down” approach. The risk-based approach developed here relies on
796 sensitivity-based analyses to a wide range of climate changes, making it scenario-neutral. However ex ante climate
797 projections are introduced in the last stage of the framework to assess the likelihood of failure.

798 The analysis of the past and current DMPs in the RM district shows a decision-making processes highly
799 heterogeneous in terms of both low-flow monitoring variable and regulatory thresholds. In reality, the WR
800 statements follow a set of rules defined in the DMPs (which can be simulated and reproduced automatically) but
801 also expert judgment or lobbying from key stakeholders - which are not accounted for in the WRL modelling
802 framework put in place here. However, the post-processing of GR6J outputs allows detecting more than 68% of
803 severe alerts (more severe than level 1), making the developed framework a useful tool. Our study is a first step
804 towards a comprehensive accounting of physical processes, but does not capture socio-economic factors, also
805 critically important and reaches out to interdisciplinary for completing the modelling framework designed here.
806 The study at the regional scale illustrates an expected difficulty to simulate accurately a regulatory framework.
807 Further improvement is not expected in enhancing hydrological models but in reproducing decision-making
808 processes. The overall performance could be improved by scrutinizing the minutes of the drought committees to
809 better understand the weight of the stakeholders in the final statement.

810 The sensitivity analysis and the related response surfaces suggest that basins located in the Southern Alps are
811 the most responsive basins to climate change and that those experiencing a high ratio P/PET are found the less
812 responsive. The classification method CART has been applied to 106 responses surfaces associated with 106

813 gauged basins and leads to four classes with different sensitivity. The key-variables known at un-modelled but
814 gauged catchments can be introduced in the decision-tree to finally predict the assignment as a first guess to one
815 of the four classes. Water managers are thus encouraged to monitor in priority and more accurately temperature
816 and/or precipitation when and where the sensitivity of their catchments is found the highest. This may mean efforts
817 to reinforce field instrumentation within these key catchments.

818 Although incomplete, the proposed framework demonstrates, as expected (see Assessment Box SPM.2 Table 1
819 in (IPCC, 2014)), a sensitivity of the DMPs to climate changes. The impact of climate change on the river flow is
820 expected to be gradual, thus offering opportunities to update, to harmonize and to adapt Drought Management
821 Plans to changes in climate conditions and water needs. As a consequence, the need for adaptation of existing
822 drought action plans could differ much from one catchment to another and should take into account intrinsic
823 sensitivity to climate change besides ‘top-down’ projections. Results also show needs to firstly adapt DMPs in
824 temperature sensitive catchments more subject to a significant increase in legally-binding restrictions in the short
825 term. In contrast, the capacity to anticipate changes in both the occurrence and severity of WR, and their
826 consequences for water management will be challenging in catchments where water restrictions are mainly driven
827 by precipitation due to their high uncertainties in future regional climate projections.

828 The risk-based approach was applied to assess the vulnerability of irrigation due to regulatory instruments under
829 modified climate. Evaluating the impact of climate change on irrigation was not the objective of the suggested
830 framework; it has been applied to estimate the likelihood of failure for irrigation at various lead times, instead.
831 Usually, a failure can be stated when irrigation water needs are not fully satisfied. This case study suggests the use
832 of a proxy obtained from a national system of compensation to define a critical threshold (maximum acceptable
833 duration with water restriction). Analysis, however, was based on limited data (one year) and a better failure
834 assessment is required using other years (e.g., 2015 and 2017). The higher the probability, the more vulnerable the
835 irrigation use within the department. Finally, socio-economic system stressors like agricultural practices,
836 population growth, water demand, etc. should be considered to highlight combinations that would lead to
837 unacceptable conditions and to assess the performance of various adaptation strategies under an extended set of
838 future climate conditions (Poff *et al.* 2016).

839 Climate response surface appears as a convenient tool for simulating and discussing future perspectives locally
840 on the basin scale or more broadly on a given management territory. For example, they can support implement
841 adaptive strategies (see - as an example - the Robust Decision Making framework suggested by Lempert and

842 Groves (2010)): response surfaces can be drawn for different adaptation scenarios combined with periodic updates
843 of DMPs including rules for defining regulatory thresholds and monitoring variables evolving over time, etc.

844 Note that all results are based on a single hydrological model, but a multi-model approach could be applied as
845 the magnitude of the rainfall-runoff response was shown vary with different hydrological models (e.g., Vidal *et*
846 *al.* 2016; Kay *et al.* 2014). Finally, an extension of the area of interest to the whole France may bring to light a
847 more complete typology of response surfaces and a wider range of sensitivity.

848 **Acknowledgments**

849 The authors thank Météo-France for providing access to the Safran database. Regional projections were obtained
850 from the DRIAS portal (<http://drias-climat.fr/>) and consulted on November 2016. Analyses were performed in R
851 (R Core Team 2016) with packages airGR (Coron *et al.* 2017), chron (James and Hornik 2017), circular (Lund *et*
852 *al.*; 2017), doParallel (Calaway *et al.* 2017), dplyr (Wickham and François 2015), ggplot2 (Wickham 2009),
853 hydroTSM (Zambrano-Bigiarini 2014), RColorBrewer (Neuwirth 2014), reshape2 (Wickham 2007), rpart
854 (Therneau *et al.* 2018), scales (Wickham 2016), stringr (Wickham 2017) and zoo (Zeileis and Grothendieck 2005).
855 The study was funded by Irstea and the French RM Water Agency.

856 **References**

857 Andrew J.T. and Sauquet E.: Climate Change Impacts and Water Management Adaptation in Two Mediterranean-
858 Climate Watersheds: Learning from the Durance and Sacramento Rivers. *Water* 2017, 9, 126, doi:
859 10.3390/w9020126, 2017.

860 Arnell N.W.: Relative effects of multi-decadal climatic variability and changes in the mean and variability of
861 climate due to global warming: future streamflow in Britain. *J. Hydrol.* 270, 19–213, 2003.

862 Barbier R., Barreteau O., and Breton C.: Management of water scarcity: between negotiated implementation of the
863 “décret sécheresse” and emergence of local agreements. *Ingénieries - EAT IRSTEA édition 2007*, 3-19, 2007.

864 Bisselink B., Bernhard J., Gelati E., Adamovic M., Guenther S., Mentaschi L. and De Roo A.: Impact of a changing
865 climate, land use, and water usage on Europe’s water resources, EUR 29130 EN, Publications Office of the
866 European Union, Luxembourg, 2018, ISBN 978-92-79-80287-4, doi:10.2760/847068, JRC110927, 2018.

867 Boé J., Terray L., Martin E., and Habets F.: Projected changes in components of the hydrological cycle in French
868 river basins during the 21st century. *Water Resour. Res.* 45 (8), W08426, doi:10.1029/2008WR007437, 2009.

869 Breiman L., Friedman J.H., Olshen R., and Stone C.J.: Classification and Regression Trees, Wadsworth, Belmont,
870 California, 1984.

871 Brekke L.D., Maurer E.P., Anderson J.D., Dettinger M.D., Townsley E.S., Harrison A., and Pruitt T.: Assessing
872 reservoir operations risk under climate change. *Water Resour. Res.*, 45, W04411, doi:10.1029/2008WR006941,
873 2009.

874 Broderick C., Murphy C., Wilby R.L., Matthews T., Prudhomme C., and Adamson, M. (2019). Using a Scenario
875 - neutral framework to avoid potential maladaptation to future flood risk. *Water Resources Research*, 55.
876 <https://doi.org/10.1029/2018WR023623>

877 Brown C., Werick W., Leger W., and Fay D.: A decision-analytic approach to managing climate risks: Application
878 to the upper great lakes. *Journal of the American Water Resources Association (JAWRA)* 47, 524–534, 2011.

879 Brown C., Ghile Y., Laverty M., and Li K.: Decision scaling: Linking bottom-up vulnerability analysis with
880 climate projections in the water sector. *Water Resour. Res.* 48, W09537, doi:10.1029/2011WR011212, 2012.

881 Brown C., Wilby R.L.: An alternate approach to assessing climate risks. *Trans. Am. Geophys. Union* 93(41), 401–
882 402, 2012.

883 Bubnová R., Hello G., Bénard P., and Geleyn J.F.: Integration of the Fully Elastic Equations Cast in the Hydrostatic
884 Pressure Terrain-Following Coordinate in the Framework of the ARPEGE/Aladin NWP System. *Monthly Weather*
885 *Review* 123 (2), 515-35, 1995.

886 Caillouet L., Vidal J.-P., Sauquet E., Devers A., and Graff B: Ensemble reconstruction of spatio-temporal extreme
887 low-flow events in France since 1871. *Hydrol. Earth Syst. Sci.* 21, 2923-2951, 2017.

888 Calaway R., Microsoft Corporation, Weston S., and Tenenbaum D.: doParallel: Foreach Parallel Adaptor for the
889 'parallel' Package. R package version 1.0.11, <https://CRAN.R-project.org/package=doParallel>, 2017.

890 Chauveau M., Chazot S., Perrin C., Bourgin P.-Y., Sauquet E., Vidal J.-P., Rouchy N., Martin E., David J., Norotte
891 T., Maugis P., and de Lacaze X: What will be the impacts of climate change on surface hydrology in France by
892 2070? *La Houille Blanche* 4, 5-15, 2013.

893 Cipriani T., Tilmant F., Branger F., Sauquet E., and Detry T. : Impact of climate change on aquatic ecosystems
894 along the Asse river network. In “Hydrology in a Changing World: Environmental and Human Dimensions”
895 (Daniell T., Ed.), *AIHS Publ.* 363, 2014, 463-468, 2014.

896 Collet L., Harrigan S., Prudhomme C., Formetta G., and Beevers L.: Future hot-spots for hydro-hazards in Great
897 Britain: a probabilistic assessment, *Hydrol. Earth Syst. Sci.*, 22, 5387-5401, [https://doi.org/10.5194/hess-22-5387-](https://doi.org/10.5194/hess-22-5387-2018)
898 2018, 2018.

899 Coron L., Thirel G., Delaigue O., Perrin C., and Andréassian V.: airGR: A Suite of Lumped Hydrological Models
900 in an R-Package. *Environmental Modelling and Software* 94, 166-171,
901 <https://doi.org/10.1016/j.envsoft.2017.05.002>, 2017.

902 Culley S., Noble S., Yates A., Timbs M., Westra S., Maier H.R., Giuliani M., and Castelletti A.: A bottom-up
903 approach to identifying the maximum operational adaptive capacity of water resource systems to a changing
904 climate. *Water Resour. Res.* 52, 6751–6768, 2016.

905 Danner A., Mohammad Safeeq G., Grant GE., Wickham C., Tullos D., and Santelmann M.V.: Scenario-Based and
906 Scenario-Neutral Assessment of Climate Change Impacts on Operational Performance of a Multipurpose
907 Reservoir. *Journal of the American Water Resources Association (JAWRA)* 53(6), 1467-1482, 2017.

908 Dayon G., Boé J., Martin E., and Gailhard J.: Impacts of climate change on the hydrological cycle over France and
909 associated uncertainties. *Comptes Rendus Geoscience* 350(4), 141-153, 2018.

910 Fronzek S., Carter T.R., and Räisänen J.: Applying probabilistic projections of climate change with impact models:
911 a case study for sub-arctic palsa mires in Fennoscandia. *Climatic Change* 99, 515–534, 2010.

912 Ghile Y.B., Taner M.Ü., Brown C., and Talbi A.: Bottom-up climate risk assessment of infrastructure investment
913 in the Niger River Basin. *Climatic Change* 122(1–2), 97–110, 2014.

914 Giorgi F.: Climate change hot-spots. *Geophys. Res. Lett.*, 33, L08707, doi:10.1029/2006GL025734, 2006.

915 Grouillet B., Fabre J., Ruelland D., and Dezetter A.: Historical reconstruction and 2050 projections of water
916 demand under anthropogenic and climate changes in two contrasted Mediterranean catchments, *J. Hydrol.*, 522,
917 684–696, 2015.

918 Guo D., Westra S., and Maier H.R.: An inverse approach to perturb historical rainfall data for scenario-neutral
919 climate impact studies. *J. Hydrol.* 556: 877-890, 2016.

920 Guo D., Westra S., and Maier H.R.: Use of a scenario-neutral approach to identify the key hydrometeorological
921 attributes that impact runoff from a natural catchment. *J. Hydrol.* <http://dx.doi.org/10.1016/j.jhydrol.2017.09.021>,
922 2017.

923 Gupta, H. V., Kling, H., Yilmaz, K., and Martinez, G. F.: Decomposition of the mean squared error and NSE
924 performance criteria: Implications for improving hydrological modelling, *J. Hydrol.*, 377, 80–91,
925 <https://doi.org/10.1016/j.jhydrol.2009.08.003>, 2009.

926 Habets F., Molénat J., Carluier N., Douez O., and Leenhardt D.: The cumulative impacts of small reservoirs on
927 hydrology: A review. *Sci. Total. Environ.*, 643, 850-867, <https://doi.org/10.1016/j.scitotenv.2018.06.188>, 2018

928 Hellwig J. and Stahl K.: An assessment of trends and potential future changes in groundwater-baseflow drought
929 based on catchment response times, *Hydrol. Earth Syst. Sci.*, 22, 6209-6224, [https://doi.org/10.5194/hess-22-](https://doi.org/10.5194/hess-22-6209-2018)
930 6209-2018, 2018.

931 Hublart P., Ruelland D., García de Cortázar-Atauri I., Gascoin S., Lhermitte S., and Ibacache A.: Reliability of
932 lumped hydrological modeling in a semi-arid mountainous catchment facing water-use changes. *Hydrol. Earth*
933 *Syst. Sci.* 20, 3691-3717, <https://doi.org/10.5194/hess-20-3691-2016>, 2016.

934 IPCC: Summary for policymakers. In: *Climate Change 2014: Impacts, Adaptation, and Vulnerability. Part A:*
935 *Global and Sectoral Aspects. Contribution of Working Group II to the Fifth Assessment Report of the*
936 *Intergovernmental Panel on Climate Change* [Field, C.B., V.R. Barros, D.J. Dokken, K.J. Mach, M.D.
937 Mastrandrea, T.E. Bilir, M. Chatterjee, K.L. Ebi, Y.O. Estrada, R.C. Genova, B. Girma, E.S. Kissel, A.N. Levy,
938 S. MacCracken, P.R. Mastrandrea, and L.L. White (eds.)]. Cambridge University Press, Cambridge, United
939 Kingdom and New York, NY, USA, pp. 1-32, 2014.

940 Jacob D., Petersen J., Eggert B., Alias A., Christensen O.B., Bouwer L.M., and Braun A.: EURO-CORDEX: New
941 high-resolution climate change projections for European impact research, *Regional environmental change* 14(2),
942 563-78, 2014.

943 Jakeman A.J., Littlewood I.G., Whitehead P.G.: Computation of the instantaneous unit hydrograph and identifiable
944 component flows with application to two small upland catchments. *J. Hydrol.*, 117, 275–300, 1990.

945 James D. and Hornik K.: chron: Chronological Objects which Can Handle Dates and Times. R package version
946 2.3-50, <https://CRAN.R-project.org/package=chron>, 2017.

947 Jiménez Cisneros B.E., Oki T., Arnell N.W., Benito G., Cogley J.G., Döll P., Jiang T., and Mwakalila S.S.:
948 Freshwater resources. In: *Climate Change 2014: Impacts, Adaptation, and Vulnerability. Part A: Global and*
949 *Sectoral Aspects. Contribution of Working Group II to the Fifth Assessment Report of the Intergovernmental Panel*
950 *on Climate Change* [Field, C.B., V.R. Barros, D.J. Dokken, K.J. Mach, M.D. Mastrandrea, T.E. Bilir, M.
951 Chatterjee, K.L. Ebi, Y.O. Estrada, R.C. Genova, B. Girma, E.S. Kissel, A.N. Levy, S. MacCracken, P.R.
952 Mastrandrea, and L.L. White (eds.)]. Cambridge University Press, Cambridge, United Kingdom and New York,
953 NY, USA, 229-269, 2014.

954 Jolliffe I.T. and Stephenson D.B.: *Forecast verification. A practitioner's Guide in Atmospheric Science.* John Wiley
955 & Sons Edition, 2003.

956 Kay A. L., Crooks S. M., and Reynard N. S.: Using response surfaces to estimate impacts of climate change on
957 flood peaks: assessment of uncertainty. *Hydrol. Process.*, 28, 5273–5287, <https://doi.org/10.1002/hyp.10000>,
958 2014.

959 Köplin N., Schädler B., Viviroli D., and Weingartner R.: Relating climate change signals and physiographic
960 catchment properties to clustered hydrological response types. *Hydrol. Earth Syst. Sci.* 16: 2267–2283, 2012.

961 Le Moine N.: Le bassin versant de surface vu par le souterrain: une voie d'amélioration des performances et du
962 réalisme des modèles pluie-débit? Ph.D. thesis. Université Pierre et Marie Curie (Paris), Cemagref (Antony), 324
963 pp, 2008

964 Lémond J., Dandin P., Planton S., Vautard R., Pagé C., Déqué M., Franchistéguy L., Geindre S., Kerdoncuff M.,
965 Li L., Moisselin J.M., Noël T., and Tourre Y.M.: DRIAS: a step toward Climate Services in France. *Adv. Sci. Res.*
966 6: 179-186, 2011.

967 Lempert R.J., and Groves D.G.: Identifying and evaluating robust adaptive policy responses to climate change for
968 water management agencies in the American west. *Technological Forecasting and Social Change* 77(6): 960-974,
969 <https://doi.org/10.1016/j.techfore.2010.04.007>, 2010.

970 Lund U., Agostinelli C., Arai H., Gagliardi A., Garcia Portugues E., Giunchi D., Irisson J.O., Pocernich M., and
971 Rotolo F.: circular: Circular Statistics. R package version 0.4-93, <https://CRAN.R-project.org/package=circular>,
972 2017.

973 Lyne V. and Hollick M.: Stochastic time variable rainfall runoff modeling. In: *Proceedings of the Hydrology and*
974 *Water Resources Symposium Berth, 1979. National Committee on Hydrology and Water Resources of the*
975 *Institution of Engineers, Australia, 89–92, 1979.*

976 Mastrandrea M.D., Heller N.E., Root T.L., and Schneider S.H.: Bridging the gap: linking climate-impacts research
977 with adaptation planning and management. *Climatic Change* 100, 87-101, 2010.

978 MEDDE - Ministère de l'Écologie et du Développement Durable (2004) Plan d'Action Sécheresse.

979 Nash J.E. and Sutcliffe J.V.: River flow forecasting through conceptual models Part I – A discussion of principles.
980 *J. Hydrol.* 10(3), 282–290, 1970.

981 Neuwirth E.: RColorBrewer: ColorBrewer Palettes. R package version 1.1-2, [https://CRAN.R-](https://CRAN.R-project.org/package=RColorBrewer)
982 [project.org/package=RColorBrewer](https://CRAN.R-project.org/package=RColorBrewer), 2014.

983 Oudin L., Hervieu F., Michel C., Perrin C., Andréassian V., Anctil F., and Loumagne C.: Which potential
984 evapotranspiration input for a lumped rainfall–runoff model?: Part 2 — towards a simple and efficient potential
985 evapotranspiration model for rainfall– runoff modelling. *J. Hydrol.* 303, 290–306, 2005.

986 Paeth H., Vogt G., Paxian A., Hertig E., Seubert S., and Jacobeit J.: Quantifying the evidence of climate change
987 in the light of uncertainty exemplified by the Mediterranean hot spot region. *Global and Planetary Change* 151,
988 144-151, 2017.

989 Paton F., Maier H., and Dandy G.: Relative magnitudes of sources of uncertainty in assessing climate change
990 impacts on water supply security for the southern Adelaide water supply system. *Water Resour. Res.* 49(3), 1643–
991 1667, 2013.

992 Perrin C., Michel C., and Andréassian V. Improvement of a parsimonious model for streamflow simulation. *J.*
993 *Hydrol.* 279, 275–289, 2003.

994 Poff N.L., Brown C.M., Grantham T.E., Matthews J.H., Palmer M.A., Spence C.M., Wilby R.L., Haasnoot M.,
995 Mendoza G.F., Dominique K.C., and Baeza A.: Sustainable water management under future uncertainty with eco-
996 engineering decision scaling. *Nature Climate Change* 6(1), 25-34, 2016.

997 Poncelet C., Merz R., Merz B., Parajka J., Oudin L., Andréassian V., and Perrin C.: Process-based interpretation
998 of conceptual hydrological model performance using a multinational catchment set. *Water Resour. Res.* 53, 7247–
999 7268, 2017.

1000 Pushpalatha R., Perrin C., Le Moine N., Mathevet T., and Andréassian V. A downward structural sensitivity
1001 analysis of hydrological models to improve low-flow simulation. *J. Hydrol.* 411, 66–76, 2011.

1002 Prudhomme C., Wilby R.L., Crooks S., Kay A.L. and Reynard N.S.: Scenario-neutral approach to climate change
1003 impact studies: Application to flood risk. *J. Hydrol.* 390(3–4), 198-209, 2010.

1004 Prudhomme C., Kay A., Crooks S., and Reynard N.: Climate change and river flooding: Climate change and river
1005 flooding: Part 1 classifying the sensitivity of British catchments. *Climatic Change* 119, 933-948, 2013a.

1006 Prudhomme C., Kay A., Crooks S., and Reynard N. Climate change and river flooding: Part 2 sensitivity
1007 characterization for British catchments and example vulnerability assessments. *Climatic Change* 119, 949–964,
1008 2013b.

1009 Quintana-Seguí P., Le Moigne P., Durand Y., Martin E., Habets F., Baillon M., Canellas C., Franchistéguy L., and
1010 Morel S.: Analysis of near-surface atmospheric variables: validation of the safran analysis over France. *J. Appl.*
1011 *Meteorol. Clim.* 47, 92–107, 2008.

1012 Radnoti G.: Comments on A Spectral Limited-Area Formulation with Time-Dependent Boundary Conditions
1013 Applied to the Shallow-Water Equations. *Monthly Weather Review* 123:2, 1995.

1014 R Core Team: R: A Language and Environment for Statistical Computing, R Foundation for Statistical Computing,
1015 Vienna, Austria, <https://www.R-project.org/>, 2016.

1016 Ray P.A. and Brown C.M. Confronting Climate Uncertainty in Water Resources Planning and Project Design: The
1017 Decision Tree Framework. Washington, DC: World Bank, 2015.

1018 Rousseeuw P.J. Silhouettes: A graphical aid to the interpretation and validation of cluster analysis. *Journal of*
1019 *Computational and Applied Mathematics* 20 (November), 53-65, 1987.

1020 Ruf T.: Le projet Aqua Domitia : intérêt et limites. *Pour*, 2012/1(213), 65-74. DOI : 10.3917/pour.213.0065.

1021 Samaniego L., Thober S., Kumar R., Wanders N., Rakovec O., Pan M., Zink M., Sheffield J., Wood E.F., and
1022 Marx, A.: Anthropogenic warming exacerbates European soil moisture droughts. *Nature Climate Change* 8(5),
1023 421-426, <https://doi.org/10.1038/s41558-018-0138-5>, 2018.

1024 Sauquet E.: Mapping mean annual river discharges: geostatistical developments for incorporating river network
1025 dependencies. *J. Hydrol.* 331, 300–314, 2006.

1026 Sauquet E., Gottschalk L., and Krasovskaia I.: Estimating mean monthly runoff at ungauged locations: an
1027 application to France. *Hydrology Research* 39(5-6), 403-423, 2008.

1028 Sauquet E. and Catalogne C.: Comparison of catchment grouping methods for flow duration curve estimation at
1029 ungauged sites in France. *Hydrol. Earth Syst. Sci.* 15, 2421–2435, 2011.

1030 Sauquet E., Arama Y., Blanc-Coutagne E., Bouscasse H., Branger F., Braud I., Brun J.-F., Cherel J., Cipriani T.,
1031 Detry T., Ducharne A., Hendrickx F., Hingray B., Krowicki F., Le Goff I., Le Lay M., Magand C., Malerbe F.,
1032 Mathevet T., Mezghani A., Monteil C., Perrin C., Poulhe P., Rossi A., Samie R., Strosser P., Thirel G., Tilmant
1033 F., and Vidal J.-P.: Water allocation and uses in the Durance River basin in the 2050s: Towards new management
1034 rules for the main reservoirs?, *La Houille Blanche* 5, 25-31, 2016.

1035 Schlef K.E., Steinschneider S., and Brown C.M.: Spatiotemporal Impacts of Climate and Demand on Water Supply
1036 in the Apalachicola-Chattahoochee-Flint Basin. *J. Water Resour. Plann. Manage.*, 2018, 144(2): 05017020, 2018.

1037 Simonovic S.P.: A new methodology for the assessment of climate change impacts on a watershed scale. *Current*
1038 *Science* 98(8), 1047-1055, 2010.

1039 Singh R., Wagener T., Crane R., Mann M.E., and Ning L.: A vulnerability driven approach to identify adverse
1040 climate and land use change combinations for critical hydrologic indicator thresholds: application to a watershed
1041 in Pennsylvania, USA. *Water Resour. Res.* 50(4), 3409–3427, 2014.

1042 Skamarock W., Klemp J., Dudhia J., Gill D., Barker D., Wang W., Huang X.-Y., and Duda M.: A description of
1043 the advanced research WRF version 3, doi:10.5065/D68S4MVH, 2008.

1044 Steinschneider S. and Brown C.M.: A semiparametric multivariate, multisite weather generator with low-
1045 frequency variability for use in climate risk assessments, *Water Resour. Res.*, 49, 7205–7220,
1046 doi:10.1002/wrcr.20528, 2013.

1047 Terray L. and Boé J.: Quantifying 21st-century France climate change and related uncertainties. *Comptes Rendus*
1048 *Geoscience*, 345, 136–149, 2013.

1049 Therneau T., Atkinson B., and Ripley B. rpart: Recursive Partitioning and Regression Trees. R package version
1050 4.1-13, <https://CRAN.R-project.org/package=rpart>, 2018.

1051 Touma D, Ashfaq M, Nayak M.A., Kao S.-C., Diffenbaugh N.S.: A multi-model and multi-index evaluation of
1052 drought characteristics in the 21st century. *J. Hydrol.*, 526, 196-207, 2015

1053 Van Loon A.F., Gleeson T., Clark J., Van Dijk A.I.J.M., Stahl K., Hannaford J., Di Baldassarre G., Teuling A.J.,
1054 Tallaksen L.M., Uijlenhoet R., Hannah D.M., Sheffield J., Svoboda M., Verbeiren B., Wagener T., Rangecroft S.,
1055 Wanders N., and Van Lanen H.A.J.: Drought in the Anthropocene, *Nature Geoscience*, 9, 89-91, 2016.

1056 Taylor K.E., Stouffer R.J., and Meehl G.A.: An overview of CMIP5 and the experiment design. *Bull. Am.*
1057 *Meteorol. Soc.* 93(4), 485-498, 2012.

1058 Valéry A., Andréassian V., and Perrin C.: 'As simple as possible but not simple': What is useful in a temperature-
1059 based snow-accounting routine? Part 2 - Sensitivity analysis of the Cemaneige snow accounting routine on 380
1060 catchments. *J. Hydrol.* 517, 1176–1187, 2014.

1061 Vidal J.-P., Martin E., Franchistéguy L., Baillon M, and Soubeyroux J.-M.: A 50-year high-resolution atmospheric
1062 reanalysis over France with the Safran system. *Int. J. Clim.* 30, 1627–1644, 2010.

1063 Vidal J.-P., Hingray B., Magand C., Sauquet E., and Ducharne A.: Hierarchy of climate and hydrological
1064 uncertainties in transient low-flow projections. *Hydrol. Earth Syst. Sci.* 20, 3651–3672, 2016.

1065 Ward J. Jr.: Hierarchical grouping to optimize an objective function. *Journal of the American Statistical*
1066 *Association* 58(301), 236-44, 1963.

1067 Whateley S., Steinschneider S., and Brown C.M.: A climate change range-based method for estimating robustness
1068 for water resources supply. *Water Resour. Res.* 50, 8944–8961, 2014.

1069 Weiß M.: Future water availability in selected European catchments: a probabilistic assessment of seasonal flows
1070 under the IPCC A1B emission scenario using response surfaces. *Nat Hazards Earth Syst Sci* 11:2163–2171, 2011.

1071 Wetterhall F., Graham L.P., Andréasson J., Rosberg J., and Yang W. Using ensemble climate projections to assess
1072 probabilistic hydrological change in the nordic region. *Natural Hazards and Earth System Sciences* 11, 2295–2306,
1073 2011.

1074 Wickham H.: ggplot2: Elegant Graphics for Data Analysis, Springer-Verlag New York, <http://ggplot2.org>, 2009.

1075 Wickham H. and Francois R. dplyr: A Grammar of Data Manipulation. R package version 0.4.3, [https://CRAN.R-](https://CRAN.R-project.org/package=dplyr)

1076 [project.org/package=dplyr](https://CRAN.R-project.org/package=dplyr), 2015.

1077 Wickham H.: scales: Scale Functions for Visualization. R package version 0.4.0, [https://CRAN.R-](https://CRAN.R-project.org/package=scales)

1078 [project.org/package=scales](https://CRAN.R-project.org/package=scales), 2016.

1079 Wickham H.: stringr: Simple, Consistent Wrappers for Common String Operations. R package version 1.2.0,

1080 <https://CRAN.R-project.org/package=stringr>, 2017.

1081 Wickham H.: stringr: Simple, Consistent Wrappers for Common String Operations. R package version 1.2.0.

1082 <https://CRAN.R-project.org/package=stringr>, 2017.

1083 Zambrano-Bigiarini M.: hydroTSM: Time series management, analysis and interpolation for hydrological

1084 modelling. R package version 0.4-2-1. <https://CRAN.R-project.org/package=hydroTSM>, 2014.

1085 Zeileis A. and Grothendieck G.: zoo: S3 Infrastructure for Regular and Irregular Time Series. Journal of Statistical

1086 Software, 14(6), 1-27. doi:10.18637/jss.v014.i06, 2005.

1087

N°	River basin	Department (department number)	Station number	Elevation (m.a.s.l.)	Area (km ²)	Regime class	NSE _{LOG}	KGES _{QRT}
1	Ouche	Côte d'Or (21)	U1324010	243	651	6	0.84	0.94
2	Bourbre	Isère (38)	V1774010	202	703	1	0.85	0.92
3	Roizonne	Isère (38)	W2335210	936	71.6	11	0.71	0.84
4	Bonne	Isère (38)	W2314010	770	143	12	0.80	0.91
5	Buëch	Hautes-Alpes (05)	X1034020	662	723	9	0.84	0.93
6	Drôme	Drôme (26)	V4214010	530	194	3	0.81	0.89
7	Drôme	Drôme (26)	V4264010	263	1150	9	0.85	0.88
8	Roubion	Drôme(26)	V4414010	264	186	9	0.83	0.93
9	Lot	Lozère (48)	O7041510	663	465	3	0.88	0.94
10	Tarn	Lozère (48)	O3011010	905	67	8	0.73	0.90
11	Tarn	Lozère (48)	O3031010	565	189	9	0.81	0.91
12	Hérault	Hérault (34)	Y2102010	126	912	8	0.83	0.88
13	Asse	Alpes de Haute-Provence (04)	X1424010	605	375	9	0.80	0.86
14	Caramy	Var (83)	Y5105010	172	215	2	0.85	0.94
15	Argens	Var (83)	Y5032010	175	485	2	0.80	0.92

1089 **Table 1: Main characteristics of the 15 catchments used for validation of water restriction simulations. Station number**
1090 **refers to the catchment number in the HYDRO database and regime class to the classification suggested by Sauquet *et***
1091 ***al.* (2008) with a gradient from Class 1- pluvial fed regime moderately contrasted to Class 12- snowmelt fed regime.**

1092

Data source	Representative Concentration Pathway			Reference
	RCP2.6	RCP4.5	RCP8.5	
ALADIN	A	A	NA	Bubnová et al. (1995). Radnoti (1995)
First quartile, median and last quartile of the ensemble EURO-CORDEX results	NA	A	A	Jacob et al. (2014)
WRF	NA	A	NA	Skamarock et al. (2008)

1093 **Table 2: Regional climate projections available in the DRIAS portal (A: available; NA: not available).**

1094

Level	Name	Water restriction							
		Recreational	Vehicle washing	Lawn watering	Swimming-pool filling	Urban washing	Irrigation	Industry	Drinking water and sanitation
0	Vigilance	×	×	×	×	×			
1	Alert	×	×	×	×	×	×	×	
2	Reinforced alert	×	×	×	×	×	×	×	
3	Crisis	×	×	×	×	×	×	×	×

1095 **Table 3: Uses affected by water restriction according to the drought severity**

1096

WR* event	WR level ≥ 1 (Benchmark)		
	<i>Yes</i>	<i>No</i>	
WR level ≥ 1 (Prediction)	<i>Yes</i>	hits	false alarms
	<i>No</i>	misses	correct negatives

1097 **Table 4: Contingency table for legally-binding restriction (WR*).**

1098

	<i>Sd</i>	Period		
		AMJJASO	JASO	MAMJ
Argens River basin (Class 1)	median	1.59	1.65	0.19
	max	3.32	3.69	1.21
Ouche River basin (Class 2)	median	0.63	0.78	1.10
	max	1.03	1.52	1.99
Roizonne River basin (Class 4)	median	1.12	1.32	0.64
	max	1.98	2.49	0.91
All	median	0.69	0.80	0.70
	max	1.45	1.70	1.24
Class 1	median	1.16	1.24	0.25
	max	2.70	2.96	1.17
Class 2	median	0.72	0.85	0.89
	max	1.45	1.81	1.43
Class 3	median	0.41	0.49	0.64
	max	0.88	0.97	1.06
Class 4	median	0.91	1.14	0.81
	max	1.78	2.15	1.28

1099 **Table 5: Summary statistics for standard deviation *Sd* of the grid for different axes.**

1100

Component of the river flow regime	Hydrological indices
Severity	Flow exceeded 95% of the time (Q_{95})
	Annual minimum 10-day daily mean low flow with a 5-year recurrence interval Annual maximum deficit below threshold Q_{95} exceeded 20% of time
Duration	Annual maximum maximal duration of the continuous sequence of zero flow within the year, exceeded on average every five years (D_{80}). Maximum duration of consecutive zero flows (D) are sampled by block maxima approach and D_{80} is defined as the empirical 80th percentile of cumulative distribution function of D
	Seasonal recession time scales (DT and D_{rec}). This duration is based on the hydrograph defined by the 1-day and 30-day moving average of the 365 long term mean daily discharges, $d=1, \dots, 365$ (Q_d and Q_{30d} , respectively). D_{rec} is defined by the time lapse between the median Q_{d50} and the 90th quantile Q_{d90} of Q_d on the falling limb of the hydrograph defined by Q_{30d} and $DT = \ln(Q_{d50}/Q_{d90})/D_{rec}$
Rate of Change	Ratio Q_{95}/Q_{50}
	Concavity index derived from flow duration curve $(Q_{10} - Q_{99})/(Q_1 - Q_{99})$ (Sauquet and Catalogne, 2011). This descriptor is a dimensionless measure of the contrast between low-flow and high-flow regimes derived from quantiles of the flow duration curve
	Baseflow index (BFI). BFI is a measure of the proportion of the baseflow component to the total river flow, calculated by the separation algorithm separation suggested by Lyne and Hollick (1979)
	Class of river flow regime based on average monthly runoff pattern defined by Sauquet <i>et al.</i> (2008) (between 1 and 12)
Frequency	Seasonality ratio (SR) $SR = Q_{95_{AMJJASON}}/Q_{95_{DJFM}}$ ($SR > 1$ for mountainous catchment) with $Q_{95_{AMJJASON}}$ and $Q_{95_{DJFM}}$ computed on seasonal flow duration curves
	Proportion of years with at least one value below Q_{95}
Timing	Mean day of first occurrence of flow below Q_{95}
	Mean and dispersion of the occurrence of flows below Q_{95} within the year (θ and r , $r \sin(\theta)$ and $r \cos(\theta)$). These two variables are circular statistics. Each day i with zero flow is converted into an angular (t_i) and represented by a unit vector with rectangular coordinates ($\cos(t_i)$; $\sin(t_i)$). The mean of the cosines and sines defines a representative vector. The value for θ is obtained by calculating the inverse tangent of the angle of the mean vector and the norm of the mean vector provides a measure of the regularity in the dates (a value close to one indicates a high concentration around θ while a value close to zero indicates no seasonality)

1102 **Table 6: Hydrological metrics considered to investigate similarity in CART.**

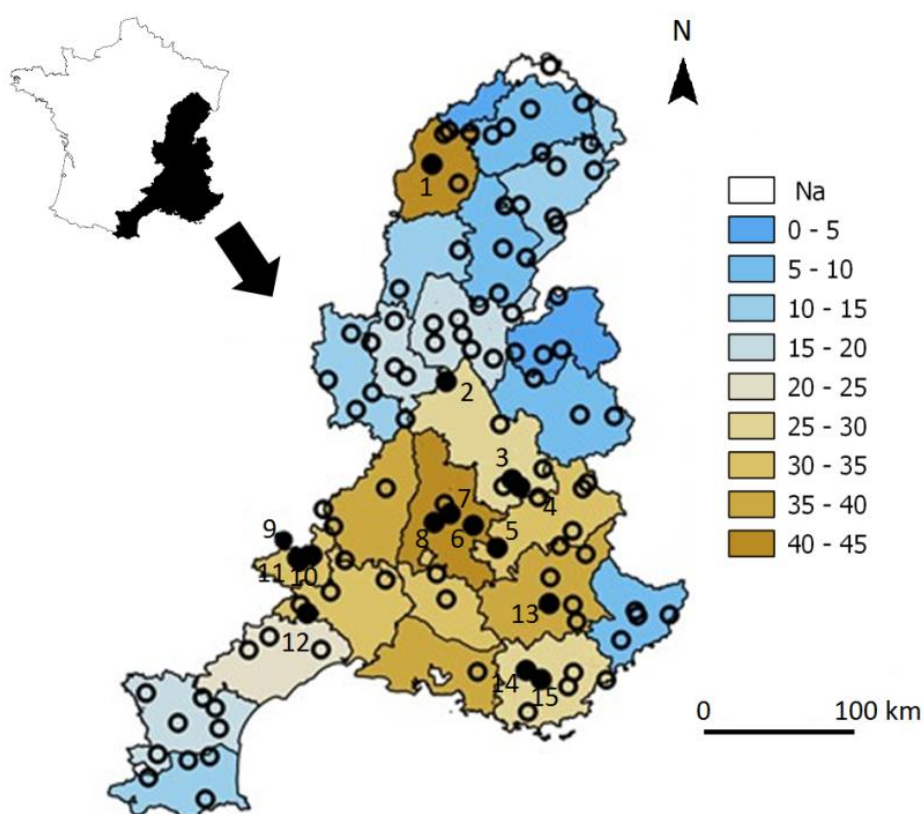
1104

Class		Number of catchments (with agricultural disaster status)	Mean $\Delta WR^*(2011)$ (with agricultural disaster status) ($\times 10$ days)	Vulnerability index VI (%)		
				2021-2050	2041-2070	2071-2100
1	All	15 (2)	-1.2 (-2.3)	6.1	11.5	6.7
2	All	44 (22)	5.0 (7.1)	6.4	11.8	21.6
	N	25 (18)	6.1 (6.2)	0	0	13
	S	19 (4)	3.4 (11.3)	14.8	27.3	32.9
3	All	38 (13)	5.4 (8.7)	1.7	4.5	7.9
	N-E	25 (4)	3.7 (3.8)	0.4	0	4.5
	S-W	13 (9)	8.5 (10.8)	4.19	13.3	14.4
4	All	9 (3)	0 (-0.7)	18.2	45.4	47.2
All		106 (40)	3.8 (6.6)	5.8	12	16.7

1105 **Table 7: Summary statistics for the mean anomaly $\Delta WR^*(2011)$ and for the measure of vulnerability VI estimated at**
 1106 **the regional scale.**

1107

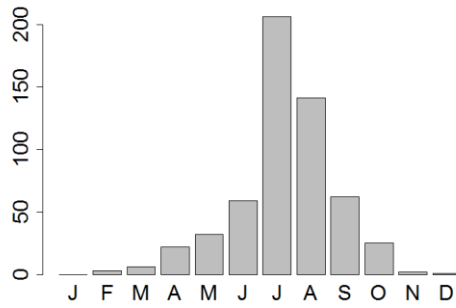
1108



1109

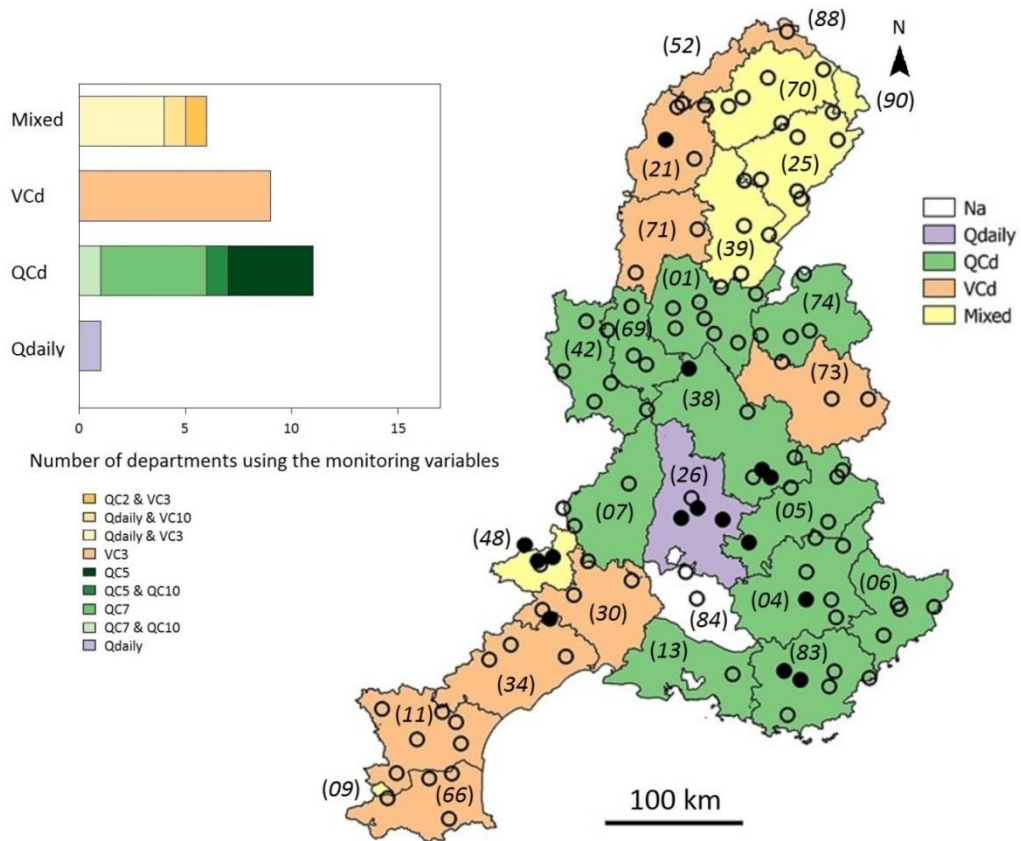
1110 **Figure 1: The Rhône-Méditerranée water district, the total number of WR decisions stated by department over the**
 1111 **period 2005-2016 and the gauged catchments \bigcirc where WR decisions are simulated (\bullet denotes the subset of the 15**
 1112 **catchments used for evaluation purposes and the figures are the related ranks presented in Table 1).**

1113



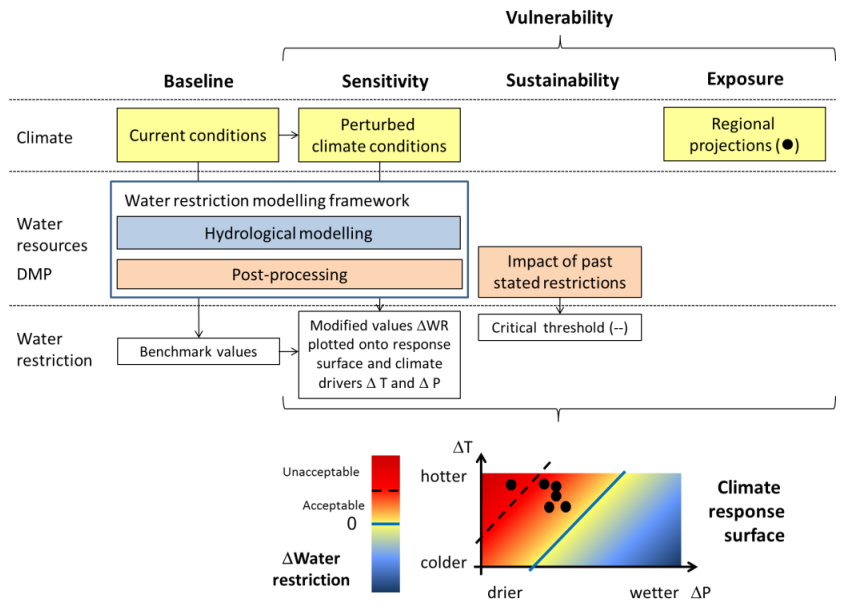
1114

1115 **Figure 2: Total number of stated WR decisions over the RM district per month over the period 2005-2016.**



1116

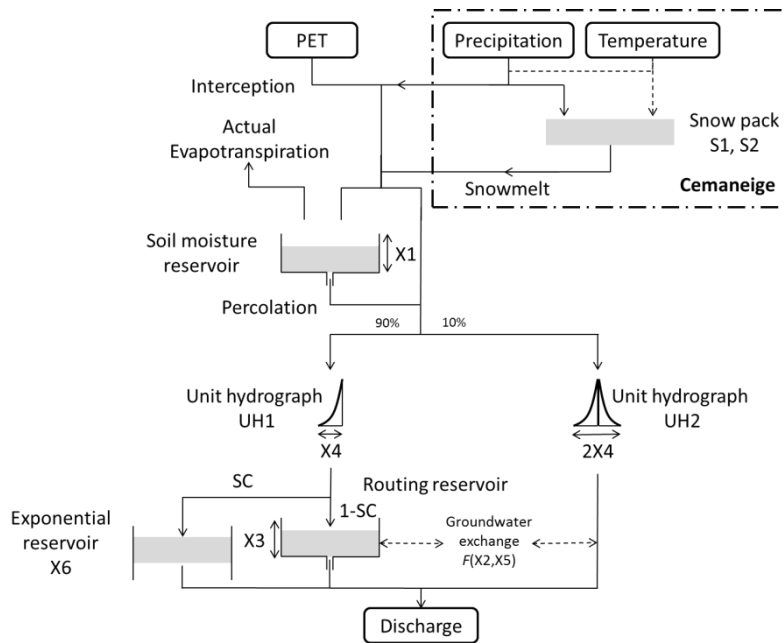
1117 **Figure 3: Low-flow monitoring variables used in the current drought management plans. *Qdaily* denotes daily**
 1118 **streamflow, *QCd* the *d*-day maximum discharge; *VCd* the *d*-day mean discharge and *Mixed* refers to combinations of**
 1119 **the aforementioned variables. Department codes are given into brackets.**



1120

1121 **Figure 4: Schematic framework of the developed approach to assess the vulnerability of the DMPs under climate**
 1122 **change.**

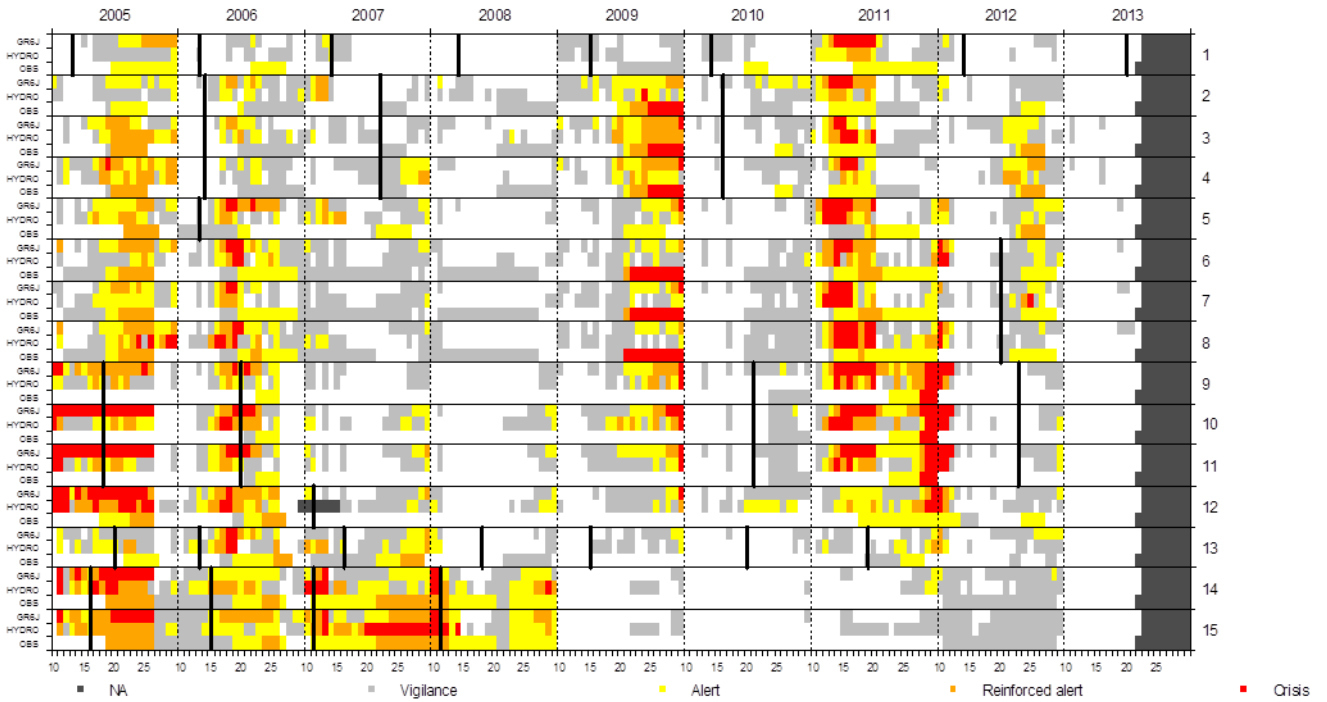
1123



1124

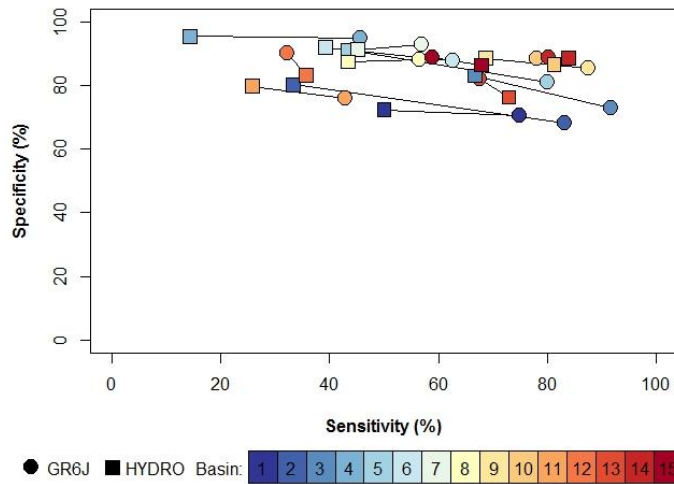
1125 **Figure 5: Schematic of the rainfall-runoff Model GR6J combined with the CemaNeige snowmelt runoff component**
 1126 **(after Pushpalatha *et al.* 2011).**

1127



1128

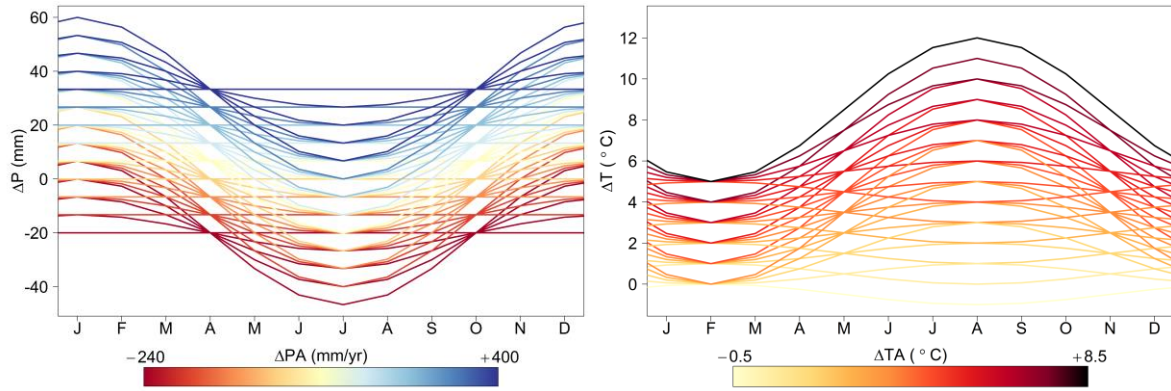
1129 **Figure 6: Observed and simulated water restriction levels considering the two sources of discharge data GR6J and**
 1130 **HYDRO for each of the 15 evaluation catchments (Table 1). The x-abcissa is divided into ten-day periods for each year**
 1131 **spanning the period April-to-October. Black segments identify updated DMPs.**



1132

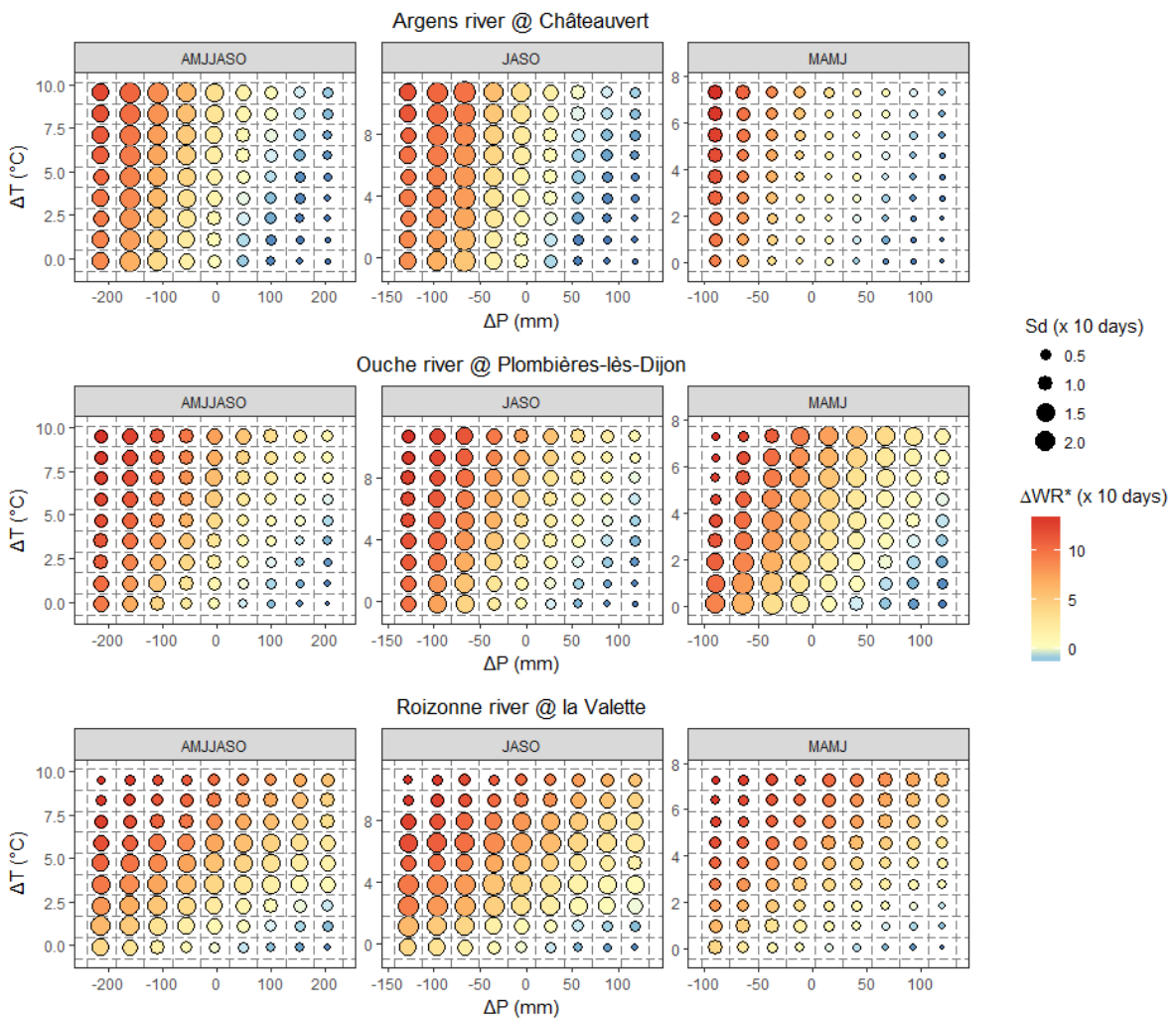
1133 **Figure 7: Skill scores obtained for the WR level model over the period 2005-2013. Each segment is related to one of the**
 1134 **15 catchments listed in Table 2. The endpoints refer to the source of discharge data (GR6J or HYDRO).**

1135



1136

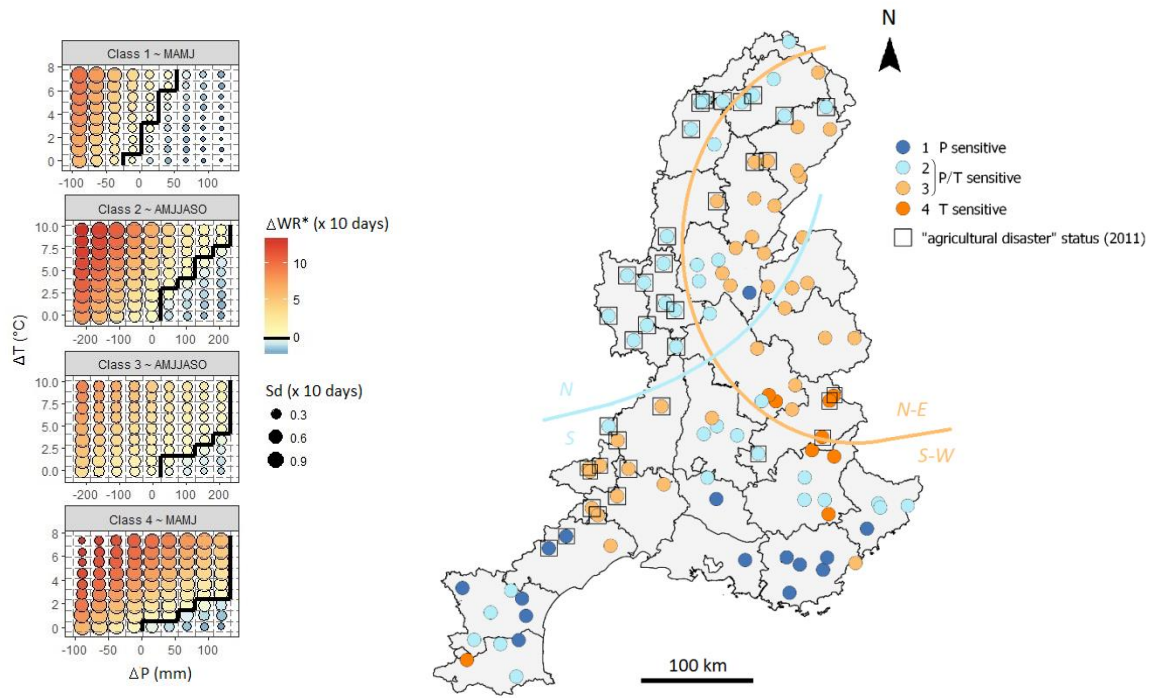
1137 **Figure 8: Monthly perturbation factors ΔP and ΔT associated with the climate sensitivity domain. The color of the line**
 1138 **is related to the intensity of the annual change ΔPA and ΔTA .**



1139

1140 **Figure 9: Climate response surface of legally-binding water restrictions level anomalies ΔWR^* for the Argens, Ouche**
 1141 **and Roizonne River basins. Each graph is obtained considering changes in mean precipitation ΔP and temperature ΔT**
 1142 **over a specific period as x- and y-axis.**

1143

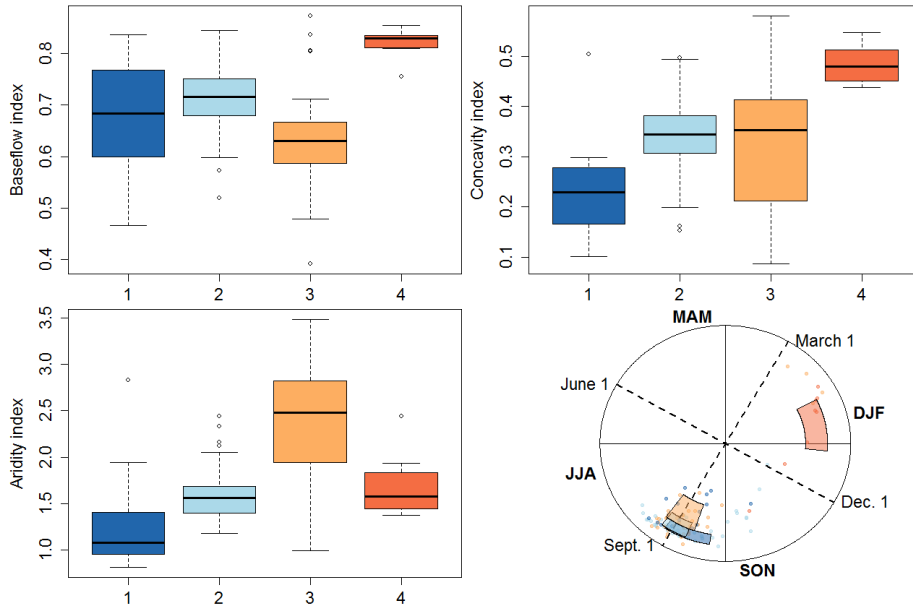


1144

1145 **Figure 10: Results of the hierarchical cluster analysis applied to the climate response surface WR^* level anomalies**

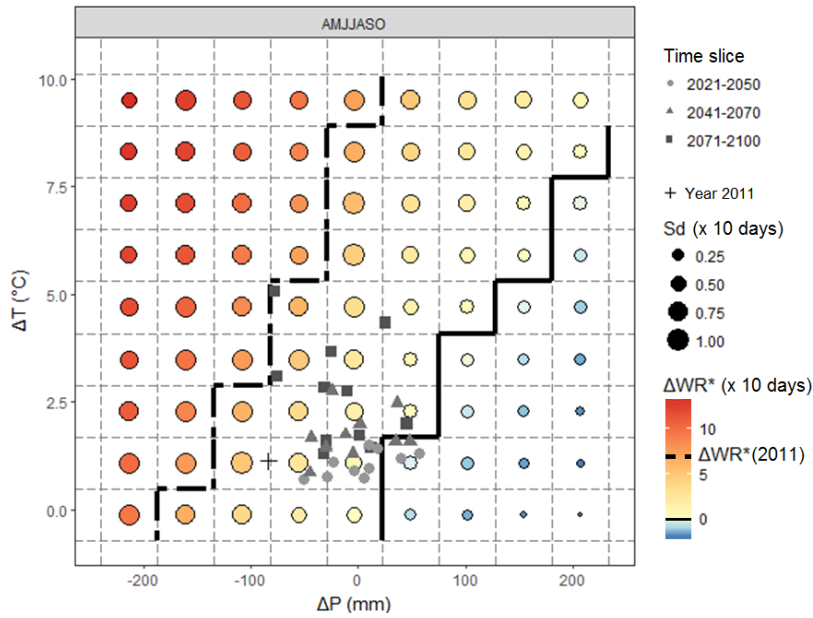
1146 **ΔWR^***

1147



1148

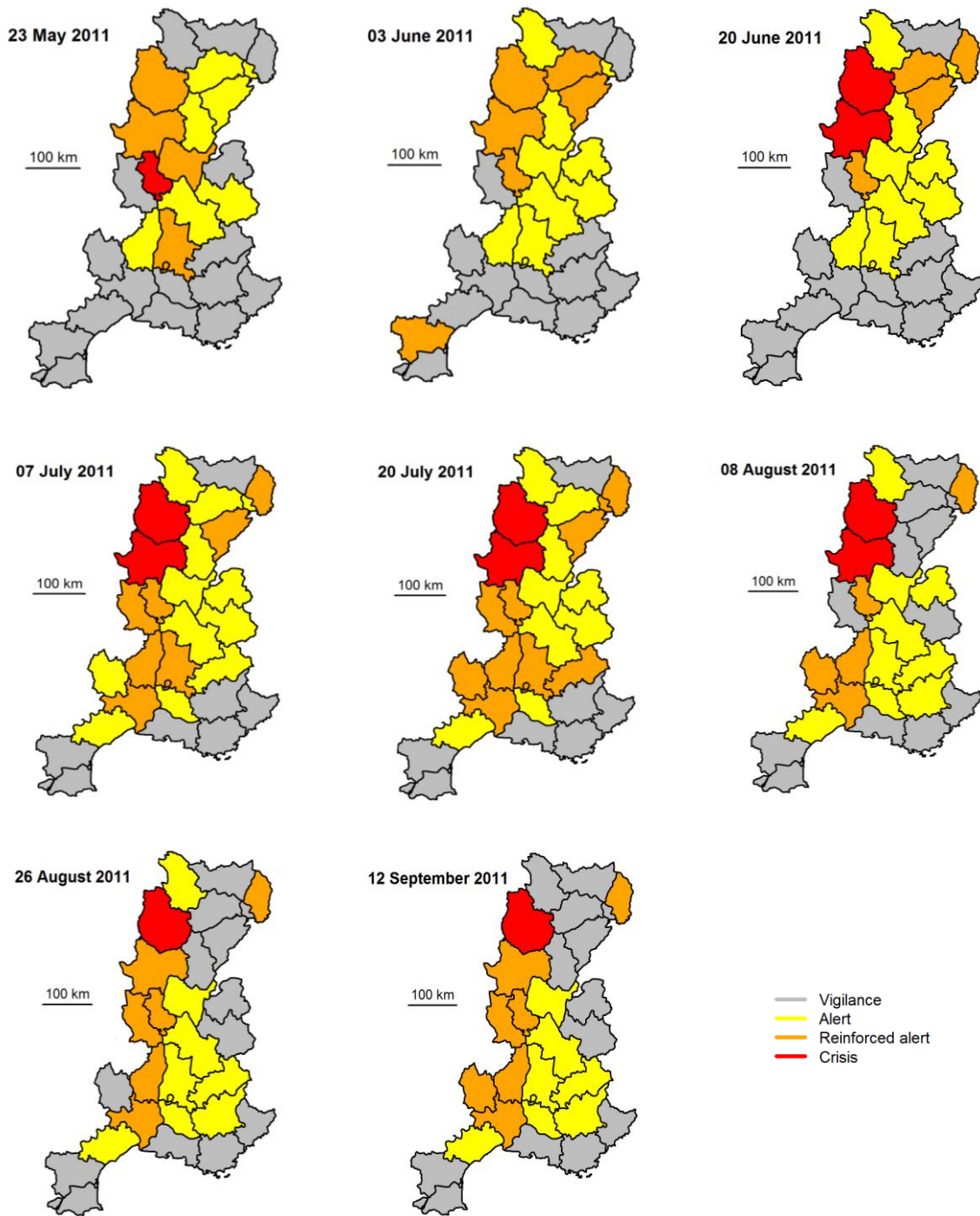
1149 **Figure 11: Statistical distribution of the discriminating factors identified by the CART algorithm (top level, top left and**
 1150 **bottom left) and the mean timing θ of daily discharge below $Q95$ and its dispersion r (bottom right). The boxplots are**
 1151 **defined by the first quartile, the median and the third quartile. The whiskers extend to 1.5 of the interquartile range;**
 1152 **open circles indicate outliers. The color is associated to the membership to one class and the name of the class is given**
 1153 **along the x-axis. The colored areas in the lower right figure are defined by the first quartile and the third quartile of r**
 1154 **and θ . Each dot is related to one gauged basin. The dotted lines indicate the start of four meteorological seasons.**



1155

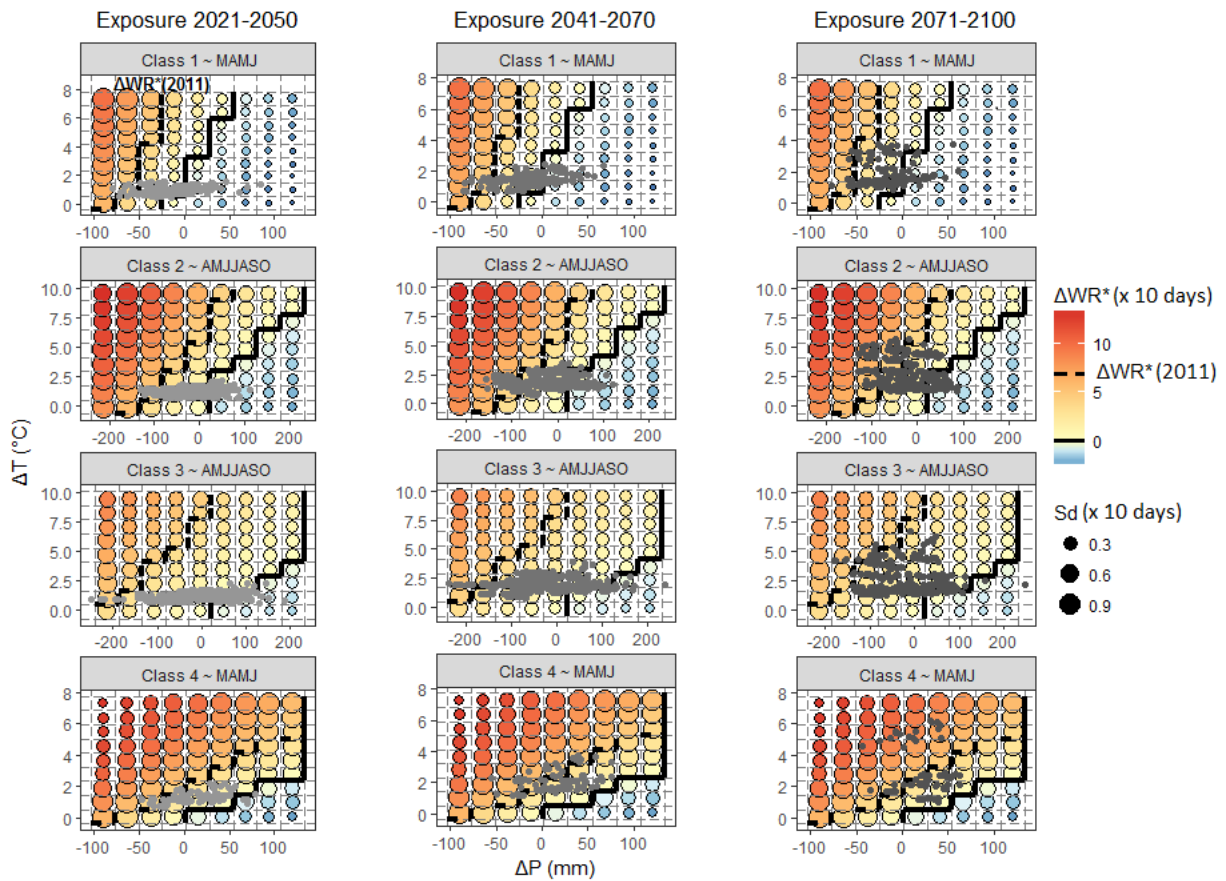
1156 **Figure 12: Climate response surface of legally-binding water restrictions level anomalies ΔWR^* for the Ouche River**
 1157 **basin including both exposure and performance characterizations.**

1158



1160 **Figure 13: Most severe water restriction level adopted at the department-level scale for several dates between May and**
 1161 **September 2011 (Source: French ministry of Ecology)**

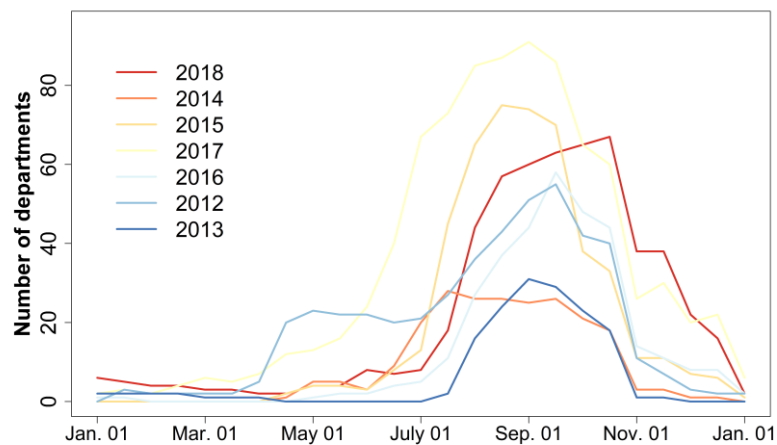
1162



1163

1164 **Figure 14: Representative climate response surfaces for each class including both exposure and performance**
 1165 **characterizations.**

1166



1167

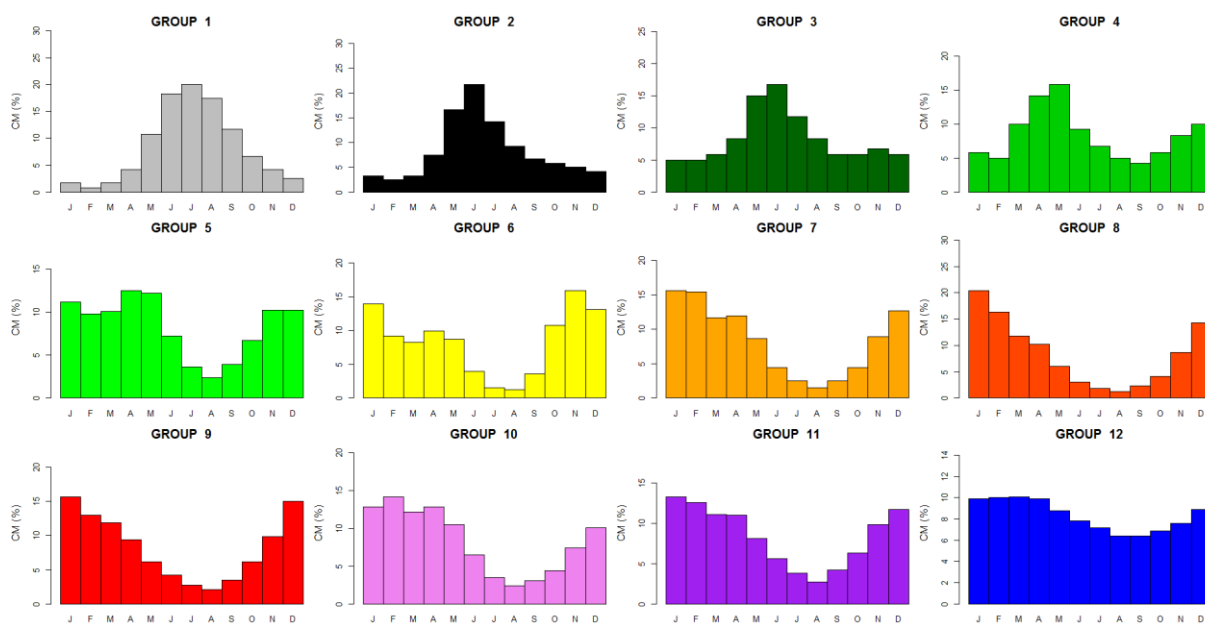
1168 **Figure 15: Number of departments with at least one sub-catchment with WR level ≥ 1 . The color of the curves is**
 1169 **associated to the annually averaged air temperature rank for France (from red to blue for the warmest (2018) to the**
 1170 **coldest year (2013)) (Sources: MétéoFrance, French ministry of Ecology).**

1171

1172 **Appendix A: Classification of river flow regime for France**

1173 Sauquet *et al.* (2008) have defined a classification based on the mean monthly runoff pattern (Fig. A1) and a
 1174 map has been published showing the assignment to one class along the main river network. The twelve
 1175 dimensionless coefficients *CM* are the twelve values of mean monthly runoff (mm) divided by the mean annual
 1176 runoff).

1177 Groups 1 to 6 are pluvial river flow regimes. The six groups mainly differ by the contrast between the maximum
 1178 and the minimum of the monthly discharges. Nearly uniform flows through most of the year (Group 1) are found
 1179 where large aquifers moderate flows whereas Group 6 is characterized by very low flow in summer, reflecting the
 1180 lack of deep groundwater storages in the catchment. Group 7 is representative of Mediterranean river flow regimes
 1181 where small rivers basins experience hot and dry summers and intense rainy events in autumn. Their runoff pattern
 1182 therefore exhibits severe low flow in summer and high flow in November. In mountainous areas, uppermost basins
 1183 display snowmelt-fed regimes (Groups 10, 11 and 12). The lower the outlet is, the lower the contributions of
 1184 snowmelt to runoff. Groups 8 to 9 are in the transition regime. The seasonal variation of streamflow is affected as
 1185 much by precipitation timing as by air temperature and topographic influences (on snowpack formation and
 1186 snowmelt timing). Typically, high flows are observed in spring.



1187
 1188 **Figure A1 : Reference dimensionless hydrographs representative of the classification of river flow regime for France**
 1189 **(after Sauquet *et al.* 2008)**